Nature of the C-Cluster in Ni-Containing Carbon Monoxide Dehydrogenases

Zhengguo Hu,[†] Nathan J. Spangler,[‡] Mark E. Anderson,[§] Jinqiang Xia,[§] Paul W. Ludden,[‡] Paul A. Lindahl,[§] and Eckard Münck*,[†]

Contribution from the Department of Chemistry, Carnegie Mellon University, Pittsburgh, Pennsylvania 15213, Department of Chemistry, Texas A & M University, College Station, Texas 77843, and Department of Biochemistry, College of Agricultural and Life Sciences, University of Wisconsin−Madison, Madison, Wisconsin 53706

Received August 17, 1995[⊗]

Abstract: The C-cluster of carbon monoxide dehydrogenase (CODH) appears to be the active site for the oxidation of CO to CO_2. We have studied with EPR and Mössbauer spectroscopy the enzymes from *Rhodospirillum rubrum* ($CODH_{Rr}$; ∼8 Fe atoms and 1 Ni atom per α) and *Clostridium thermoaceticum* ($CODH_{Ct}$; ∼12 Fe atoms and 2 Ni atoms per $\alpha\beta$). The study of $CODH_{Rr}$ offers two advantages. First, the enzyme lacks the A-cluster responsible for the synthase activity of $CODH_{Ct}$. Second, a Ni-deficient protein (Ni-deficient $CODH_{Rr}$) containing all Fe components of the holoenzyme can be isolated. The holoenzymes of both species can be prepared in a state for which the C-cluster exhibits the so-called $g_{av} = 1.82$ EPR signal (C_{red1}); the spectra of Ni-deficient $CODH_{Rr}$ do not exhibit this signal. Our results are as follows: The Mössbauer data show that all iron atoms of Ni-deficient $CODH_{Rr}$ belong to two $[Fe_4S_4]^{1+/2+}$ clusters. The so-called B-cluster, which functions in electron transfer, is diamagnetic in the $[Fe_4S_4]^{2+}$ state, B_{ox}, and exhibits an $S = 1/2$ ($g = 1.94$) EPR signal in the $[Fe_4S_4]^{+}$ state, B_{red}. The spectroscopic properties of the B-cluster are the same in Ni-deficient, holo-$CODH_{Rr}$ and $CODH_{Ct}$. The precursor to the C-cluster of Ni-deficient $CODH_{Rr}$, labeled C*, is diamagnetic in the $[Fe_4S_4]^{2+}$ state, but has an $S = 3/2$ spin in the $[Fe_4S_4]^{+}$ form. Upon incorporation of Ni, the properties of the C*-cluster change substantially. At $E'_m = -110$ mV, the C-cluster undergoes a 1-electron reduction from the oxidized state, C_{ox}, to the reduced state, C_{red1}, which exhibits the $g_{av} = 1.82$ EPR signal. A study of a sample poised at −300 mV shows that this signal originates from an $S = 1/2$ $[Fe_4S_4]^{+}$ cluster. In this state, the cluster has a distinct subsite, ferrous component II (FCII), having $\Delta E_Q = 2.82$ mm/s and $\delta = 0.82$ mm/s; these parameters suggest a pentacoordinate site somewhat similar to subsite Fe_a of the Fe_4S_4 cluster of active aconitase. The same values for ΔE_Q and δ were observed for $CODH_{Ct}$. Upon addition of CN^-, a potent inhibitor of CO oxidation, the ΔE_Q of FCII of $CODH_{Ct}$ changes from 2.82 to 2.53 mm/s, suggesting that CN^- binds to the FCII iron. The Mössbauer studies of $CODH_{Rr}$ showed that only ∼60% of the C-clusters were capable of attaining the C_{red1} state; the remainder were C_{ox} (or C^*_{ox}). For the Mössbauer sample, the EPR spin concentration of the $g_{av} = 1.82$ signal was ∼65% of that determined for the $g = 1.94$ signal of B_{red} of the fully reduced sample, a result consistent with the ∼60% obtained from Mössbauer spectroscopy. When $CODH_{Rr}$ was reduced with CO or dithionite, a fraction of the C-clusters developed a signal similar to the $g_{av} = 1.86$ signal (C_{red2}) of $CODH_{Ct}$. The Mössbauer and EPR spectra of dithionite-reduced $CODH_{Rr}$ show that a large fraction of the C-centers are in a state for which the $[Fe_4S_4]^{+}$ cluster has $S = 3/2$. While the assumption of an $[Fe_4S_4]^{+}$ cluster with an aconitase-type subsite electronically isolated from the Ni site can explain the g values of the $g_{av} = 1.82$ signal and the absence of ^{61}Ni hyperfine interactions, published resonance Raman and EPR data suggest that the Ni site may be electronically linked to the Fe−S moiety of the C-cluster. We present a model that considers a weak exchange interaction (effective coupling constant j) between an $S = 1$ Ni^{II} site (zero-field splitting, D) and the $S = 1/2$ ground state of the $[Fe_4S_4]^{+}$ cluster. This model suggests $|j| < 2$ cm^{-1}, accounts for the g values of C_{red1}, and provides an explanation for the unusual g values ($g_{av} \approx 2.16$) reported by S. W. Ragsdale and co-workers for the adducts of $CODH_{Ct}$ with thiocyanate and cyanate. The coupling model is consistent with ^{61}Ni EPR studies of CODH.

Carbon monoxide dehydrogenases constitute one of only four known classes of naturally-occurring Ni-containing enzymes.[1,2] They are found in acetogenic, methanogenic, photosynthetic, and sulfate-reducing bacteria, where they catalyze the reversible oxidation of CO to CO_2.[3,4] These enzymes contain Ni and Fe−S clusters and are inactivated by oxygen and inhibited by cyanide. The enzymes from acetogens also catalyze the synthesis of acetyl-CoA in the so-called Wood/Ljungdahl pathway of autotrophic growth,[3,5] and those from methanogens participate in the synthesis of methane from acetic acid (acetoclastic methanogenesis).[4,6] However, our focus here will be on their CO/CO_2 redox activity and requisite metal clusters.

The enzyme from the acetogen *Clostridium thermoaceticum* ($CODH_{Ct}$) has been studied in the most detail.[7] It has an $\alpha_2\beta_2$

* To whom correspondence should be addressed at the Department of Chemistry, Carnegie Mellon University, 4400 5th Ave., Pittsburgh, PA 15213. Phone: 412-268-5058. Fax: 412-268-1061. E-mail: em40+@andrew.cmu.edu.

[†] Carnegie Mellon University.

[§] Texas A & M University.

[‡] University of Wisconsin−Madison.

[⊗] Abstract published in *Advance ACS Abstracts,* December 15, 1995.

(1) *Biochemistry of Nickel*; Hausinger, R. P., Ed.; Plenum Press: New York. 1993.

(2) *The Bioinorganic Chemistry of Nickel*; Lancaster, J. R., Ed.; VCH: New York, 1988.

(3) *Acetogenesis*; Drake, H. L., Ed.; Chapman & Hall: New York, 1994.

(4) *Methanogenesis*; Ferry, J. G., Ed.; Chapman & Hall: New York, 1993.

(5) Wood, H. G.; Ljungdahl, L. G. In *Variations in Autotrophic Life*; Shively, J. M., Barton, L. L., Eds.; Academic Press: London, 1991; pp 201−250.

(6) Ferry, J. G. *J. Bacteriol.* **1992**, *174*, 5489−5495.

0002-7863/96/1518-0830$12.00/0

Table 1. Summary of EPR Signals from the B- and C-Clusters of Ni-Containing CODH's

organism	$E^{\circ\prime}$ (B_{ox}/B_{red})	$E^{\circ\prime}$ (C_{ox}/C_{red1})	g values (B_{red})	g values (C_{red1})	g_{av} (C_{red1})	g values (C_{red2})	g_{av} (C_{red2})	ref
C. thermoaceticum	−440	−220	2.04, 1.94, 1.90	2.01, 1.81, 1.65	1.82	1.97, 1.87, 1.75	1.86	22
R. rubrum	−418	−110	2.04, 1.93, 1.89	2.03, 1.88, 1.71	1.87	1.97, 1.87, 1.75[a]	1.86	42, 52
M. thermophilia	−444	−154	2.04, 1.93, 1.89	2.02, 1.88, 1.71	1.87	−, −, 1.79		36
M. barkeri	−390	−35	2.05, 1.94, 1.90	2.01, 1.91, 1.76	1.89	−, −, 1.73		37
M. soehngenii	−410	−230	2.05, 1.94, 1.89[b]	2.00, 1.89, 1.72	1.87	not reported		35

[a] This work. [b] The *M. soehngenii* enzyme may have two clusters yielding a $g = 1.94$ signal; see ref 35.

quaternary structure with a molecular mass of 310 000 Da.[8,9] Each $\alpha\beta$ dimer contains 2 Ni atoms, 11−13 Fe atoms, and ∼14 sulfide ions. SDS induces the dissociation of the enzyme into subunits.[10] The isolated β subunit is not stable and is largely devoid of metal ions. Isolated α is quite stable and contains 1 Ni atom and 4 Fe atoms.[11] The irons are organized into an $[Fe_4S_4]^{2+/1+}$ cluster which has a cluster spin $S = 3/2$ in its reduced state and exhibits EPR features in the range $g = 4-6$. The Ni and the Fe_4S_4 cluster appear to be decomposition products of the *A-cluster*,[11] a novel Ni−Fe−S center that serves as the active site for acetyl-CoA synthesis. The structure of the A-cluster is unknown, but the iron components have features of Fe_4S_4 clusters.[12] The A-cluster can exist in two oxidation states, with $E^{\circ\prime} = -530$ mV vs NHE.[6,13,14] In the presence of CO, the cluster affords an $S = 1/2$ state that yields the so-called *NiFeC* EPR signal.[15−17]

The CO oxidation/CO_2 reduction activity is catalyzed at another active site in the enzyme called the *C-cluster*.[18−21] The C-cluster is stable in three states (see Table 1), namely, a diamagnetic oxidized state (C_{ox}), a one-electron-reduced $S = 1/2$ state that exhibits an EPR signal with g values at 2.01, 1.81, and 1.65 ($g_{av} = 1.82$; C_{red1}), and another $S = 1/2$ state that exhibits g values at 1.97, 1.87, and 1.75 ($g_{av} = 1.86$; C_{red2}).[22] C_{red2} replaces C_{red1} as solution potentials are lowered. C_{red2} may be isoelectronic with C_{red1}, or it may be two-electrons more reduced. The midpoint potential for the C_{ox}/C_{red1} couple is −220 mV, while the C_{red1}/C_{red2} conversion occurs near the redox potential of the CO/CO_2 couple (−520 mV).

Cyanide is a potent, tight-binding inhibitor of CO oxidation that binds to the C_{red1} form of the C-cluster.[18,19] CN^--inhibited enzyme can be reactivated by incubation in CO. The mechanism effecting this reactivation remains to be established, but CO appears to bind to a site other than that to which CN^- binds.[18,19]

The $g_{av} = 1.82$ and 1.86 signals have unusually low spin concentrations, quantifying to only 0.2−0.3 spin/$\alpha\beta$, rather than 1.0 spin/$\alpha\beta$ as would be expected for isolated $S = 1/2$ spin systems, assuming one C-cluster per $\alpha\beta$.[20] The cause for these low values has not been determined (they do not appear to arise from incomplete reduction or errors in protein concentration), and similarly low intensities are observed for the NiFeC signal and all of the enzyme's other EPR signals.[12,23]

The structure of the C-cluster is unknown, but its Mössbauer features suggest that it contains an Fe−S cluster.[12] The frequency of a Raman-sensitive vibration from the C-cluster changes when different Ni isotopes are used in samples, indicating that Ni is also part of the C-cluster.[24]

Besides the Fe_4S_4 cluster in the α metallosubunit, native $CODH_{Ct}$ contains another $[Fe_4S_4]^{2+/1+}$ cluster known as the *B-cluster*. The B-cluster is diamagnetic when oxidized and has $S = 1/2$ when reduced ($E^{\circ\prime} = -440$ mV; Table 1).[12,22] B_{red} exhibits either of two $g = 1.94$ EPR signals having the same g values but different line widths. Together, these signals quantify to 0.64 ± 0.14 spin/$\alpha\beta$. B_{red} also exhibits a quadrupole doublet, called *ferrous component I*, with parameters ($\Delta E_Q = 2.2$ mm/s, $\delta = 0.61$ mm/s) typical of the ferrous pair of an $[Fe_4S_4]^+$ cluster.[12] The B-cluster apparently functions to transfer electrons between the C-cluster and external redox agents.[19,20]

About 9% of the absorption of the high-temperature Mössbauer spectra of reduced $CODH_{Ct}$ (i.e., 1 Fe atom/$\alpha\beta$) belongs to a quadrupole doublet called *ferrous component II* (FCII).[12] FCII was proposed to be an autonomous species because it seemed to develop at potentials more negative than that required to reduce the C-cluster and more positive than those required to reduce the A- and B-clusters. FCII behaves as though it belongs to a half-integer spin system rather than the integer spin system expected for a high-spin ferrous ion. This was rationalized by suggesting that the high-spin ferrous FCII ion was coupled to another paramagnet such as Ni^{I} or Ni^{III}.[12]

The enzyme from *Rhodospirillum rubrum* ($CODH_{Rr}$) is simpler than $CODH_{Ct}$. It is a monomer ($M_r = 61\,800$) containing 1 Ni atom and 7−9 Fe atoms,[25] and it catalyzes only the reversible oxidation of CO to CO_2. Yet, $CODH_{Rr}$ has many properties in common with $CODH_{Ct}$. Its amino acid sequence is 46% identical to the β subunit of $CODH_{Ct}$.[26] When reduced, $CODH_{Rr}$ exhibits two EPR signals, one $g = 1.94$ signal and the other with g values at 2.03, 1.88, and 1.71. The former signal almost certainly arises from an $[Fe_4S_4]^{2+/1+}$ cluster similar to the B-cluster of $CODH_{Ct}$, while the latter appears to arise from a cluster similar to the C-cluster of $CODH_{Ct}$ (Table 1). We will assume that these similarities reflect from similar

(7) Ragsdale, S. W. *CRC Crit. Rev. Biochem. Mol. Biol.* **1991**, *26*, 261−300.
(8) Xia, J.; Sinclair, J. F.; Baldwin, T. O.; Lindahl, P. A. *Biochemistry*, in press.
(9) Morton, T. A.; Runquist, J. A.; Ragsdale, S. W.; Shanmugasundaram, T.; Wood, H. G.; Ljungdahl, L. G. *J. Biol. Chem.* **1991**, *266*, 23824−23828.
(10) Xia, J.; Lindahl, P. A. *Biochemistry* **1995**, *34*, 6037−6042.
(11) Xia, J.; Dong, J.; Wang, S.; Scott, R. A.; Lindahl, P. A. *J. Am. Chem. Soc.* **1995**, *117*, 7065−7070.
(12) Lindahl, P. A.; Ragsdale, S. W.; Münck, E. *J. Biol. Chem.* **1990**, *265*, 3880−3888.
(13) Gorst, C. M.; Ragsdale, S. W. *J. Biol. Chem.* **1991**, *266*, 20687−20693.
(14) Shin, W.; Lindahl, P. A. *Biochemistry* **1992**, *31*, 12970−12875.
(15) Ragsdale, S. W.; Ljungdahl, L. G.; DerVartanian, D. V. *Biochem. Biophys. Res. Commun.* **1982**, *114*, 658−663.
(16) Ragsdale, S. W.; Ljungdahl, L. G.; DerVartanian, D. V. *Biochem. Biophys. Res. Commun.* **1983**, *115*, 658−665.
(17) Ragsdale, S. W.; Wood, H. G.; Antholine, W. E. *Proc. Natl. Acad. Sci. U.S.A.* **1985**, *82*, 6811−6814.
(18) Anderson, M. E.; DeRose, V. J.; Hoffman, B. M.; Lindahl, P. A. *J. Am. Chem. Soc.* **1993**, *24 115*, 12204−12205.
(19) Anderson, M. E.; Lindahl, P. A. *Biochemistry* **1994**, *33*, 8702−8711.
(20) Kumar, M.; Lu, W.-P.; Liu, L.; Ragsdale, S. W. *J. Am. Chem. Soc.* **1993**, *115*, 11646−11647.
(21) Seravalli, J.; Kumar, M.; Lu, W.-P.; Ragsdale, S. W. *Biochemistry* **1995**, *34*, 7879−7888.
(22) Lindahl, P. A.; Münck, E.; Ragsdale, S. W. *J. Biol. Chem.* **1990**, *265*, 3873−3879.
(23) Shin,W.; Lindahl, P. A. *Biochim. Biophys. Acta* **1993**, *1161*, 317−322.
(24) Qiu, D.; Kumar, M.; Ragsdale, S. W.; Spiro, T. G. *J. Am. Chem. Soc.* **1995**, *117*, 2653−2654.
(25) Bonam, D. Ludden, P. W. *J. Biol. Chem.* **1987**, *262*, 2980−2987.
(26) Kerby, R. L.; Hong, S. S.; Ensign, S. A.; Coppoc, L. J.; Ludden, P. W.; Roberts, G. P. *J. Bacteriol.* **1992**, *174*, 5284−5294.

clusters, and use a common nomenclature to describe them. The Ni is reported from EXAFS to be coordinated by 2 S donors at 2.23 Å and 2−3 N/O atoms at 1.87 Å in a distorted pentacoordinate or tetrahedral geometry.[27] The iron atoms appear to be organized as an Fe−S cluster. EXAFS studies suggest that the Ni is not incorporated into the corner of the cluster.[27] The effect of CN^- on the two enzymes appears to be essentially the same; CN^- is a tight-binding inhibitor of CO oxidation by $CODH_{Rr}$ that shifts the C_{red1} signal and apparently binds to the C-cluster.[23,33]

By growing *R. rubrum* under a CO atmosphere in media devoid of Ni, $CODH_{Rr}$ can be prepared in a *Ni-deficient* form that contains all of the iron atoms of holo-$CODH_{Rr}$.[29,30] Ni-deficient $CODH_{Rr}$ does not exhibit activity or the C_{red1} signal, and it does not bind CN^-. Adding Ni to reduced Ni-deficient $CODH_{Rr}$ restores catalytic activity, the C_{red1} signal, and the ability to bind CN^-. Ensign *et al*. concluded that the added Ni inserts into Ni-deficient $CODH_{Rr}$, and that Ni is the site of CO and CN^- binding.[29,30]

The similarities between $CODH_{Rr}$ and $CODH_{Ct}$ also extend to the three methanogenic CO dehydrogenases examined so far (*Methanosarcina thermophilia*, *Methanosarcina barkeri*, and *Methanothrix soehngenii*). These enzymes share similar EPR signals, redox potentials, and CN^- inhibition properties with $CODH_{Rr}$ and $CODH_{Ct}$ (Table 1).[31−39] CO also affects their C_{red1} states and reverses CN^- inhibition. Thus, with regards to CO oxidation every known Ni-containing CODH appears to contain a common assembly of clusters, and use a common mechanism for catalyzing CO oxidation/CO_2 reduction. The requisite clusters include a novel Ni- and Fe-containing C-cluster active site, and an Fe_4S_4 B-cluster that serves to transfer electrons between the C-cluster and external redox agents.

For nearly a decade, the three groups collaborating here have been attempting to determine the structure of the C-cluster, and thereby gain insight into the mechanism of catalysis. We have recently combined our efforts. The Mössbauer and EPR evidence reported here shows that the C-cluster is an Fe_4S_4 cluster that is probably linked through a bridging ligand to a Ni^{II} site. FCII represents a unique iron in this cluster, coordinated by 5−6 donors, and is the probable site of CN^- binding. Moreover, we show that the substoichiometric values for the spin quantitations of the $g_{av} = 1.82$ signal arise because the C-clusters can exist in two different forms.

Materials and Methods

Cell Growth and Purification of $CODH_{Rr}$. *R. rubrum* cells were grown on media enriched in ^{57}Fe, and under conditions that afforded either holo-$CODH_{Rr}$ or Ni-deficient $CODH_{Rr}$.[29] Two batches of $CODH_{Rr}$ and one batch of Ni-deficient $CODH_{Rr}$ were purified as described.[25,29,41] Batch 1 of $CODH_{Rr}$ was ∼90% pure in protein according to densitometry analysis of coomassie stained SDS−PAGE gels. It had a specific activity of 5090 units/mg (1 unit = 1 μmol of CO oxidized/min) and contained 6.5 iron atoms/mol of protein and 10 nickel atoms/mol of protein as determined by atomic absorption spectrometry. If the 10% protein contaminants were free of Fe, batch 1 would have ∼7.2 Fe atoms/mol of $CODH_{Rr}$. (We are uncertain why this batch contained so much Ni, except that it appears to originate from a gray-black contaminant. We have no evidence that the excess Ni is bound to $CODH_{Rr}$. As far as we can tell, the presence of excess Ni in this batch had no effect on the spectroscopic properties of the enzyme; see also ref 53 below.) Batch 2 of $CODH_{Rr}$ had a specific activity of 4800 units/mg and contained 7.2 Fe atoms/mol and 0.9 Ni atom/mol. The preparation of Ni-deficient $CODH_{Rr}$ had an activity of 94 units/mg and contained 5.2 Fe atoms/mol and 0.03 Ni atom/mol. Protein concentrations of $CODH_{Rr}$ samples were determined by the bicinchininic acid colorometric method[42] using grade A bovine serum albumin as the standard. CO oxidation activity was determined by the CO-dependent methylviologen reduction assay as previously described.[41]

C. thermoaceticum cells were grown as described,[43] except that the yeast extract/tryptone solution was passed through a Chelex (BioRad) column, glassware was soaked in dilute acid prior to use, and the medium was enriched in ^{57}Fe (10 mg/17 Liter carboy). Two batches of $CODH_{Ct}$ were purified as described.[23,44,45] Batches 1 and 2 had 220 and 246 units/mg of CO oxidation activity, respectively. Batch 1 had 0.07 unit/mg of CO/acetyl-CoA exchange activity.

Preparation of $CODH_{Rr}$ Samples. $CODH_{Rr}$ samples were reduced with dithionite and then passed through a G-25 column to render them dithionite-free. The samples thus prepared were anaerobically poised at −15 and −300 mV vs NHE in an electrochemical cell[46] containing a silver/silver chloride reference electrode, a platinum counter electrode, and a gold working electrode. For each sample, the cell was rendered anaerobic by several cycles of vacuum/scrubbed argon. An anaerobic solution of buffer of 100 mM MOPS (3-(*N*-morpholino)propanesulfonic acid) at pH 7.3, containing 0.2 mM KCl and 0.1 mM each of the appropriate mediators, was added to the cell followed by several more cycles of vacuum/argon before an equal volume of anaerobic, dithionite-free MOPS buffer containing $CODH_{Rr}$ was added. The redox potential was established with an Electrosynthesis Model 410 potentiostatic controller, and once equilibrated (i.e., <2 mV/min drift), the redox-poised solution was anaerobically transferred into a Mössbauer cup and EPR tube, and frozen in liquid N_2. Fully-reduced $CODH_{Rr}$ and fully-reduced Ni-deficient $CODH_{Rr}$ were prepared in an anearobic box containing less than 1 ppm oxygen (Vacuum/Atmospheres Dri-Lab glovebox, Model HE-493) by adding dithionite (ca. 1 and 2 mM final concentrations, respectively). Oxidized Ni-deficient $CODH_{Rr}$ as well as a second oxidized $CODH_{Rr}$ sample was prepared in the same box by removing dithionite using a Sephadex G25 column equilibrated in 100 mM MOPS buffer, and adding thionin (ca. 2 mM final concentration). Ni-depleted $CODH_{Rr}$ was activated by binding it to a DE-52 column, and

(27) Tan, G. O.; Ensign, S. A.; Ciurli, S.; Scott, M. J.; Hedman, B.; Holm, R. H.; Ludden, P. W.; Korszun, Z. R.; Stephens, P. J.; Hodgson, K. O. *Proc. Natl. Acad. Sci. U.S.A.* **1992**, *89*, 4427−4431.

(28) Ensign, S. A.; Hyman, M. R.; Ludden, P. W. *Biochemistry* **1989**, *28*, 4973−4979.

(29) Ensign, S. A.; Bonam, D.; Ludden, P. W. *Biochemistry* **1989**, *28*, 4968−4973.

(30) Ensign, S. A.; Campbell, M. J.; Ludden, P. W. *Biochemistry* **1990**, *29*, 2162−2168.

(31) Jetten, M. S. M.; Hagen, W. R.; Pierik, A. J.; Stams, A. J. M.; Zehnder, A. J. B. *Eur. J. Biochem.* **1991**, *195*, 385−391.

(32) Krzycki, J. A.; Prince, R. C. *Biochim. Biophys. Acta* **1990**, *1015*, 53−60.

(33) Grahame, D. A. *J. Biol. Chem.* **1991**, *266*, 22227−22233.

(34) Terlesky, K. C.; Barber, M. J.; Aceti, D. J.; Ferry, J. G. *J. Biol. Chem.* **1987**, *262*, 15392−15395.

(35) Jetten, M. S. M.; Pierik, A. J.; Hagen, W. R. *Eur. J. Biochem.* **1991**, *202*, 1291−1297.

(36) Lu, W.-P.; Jablonski, P. E.; Rasche, M.; Ferry, J. G.; Ragsdale, S. W. *J. Biol. Chem.* **1994**, 9736−9742.

(37) Krzycki, J. A.; Mortenson, L. E.; Prince, R. C. *J. Biol. Chem.* **1989**, *264*, 7217−7221.

(38) Smith, E. T.; Ensign, S. A.; Ludden, P. W.; Feinberg, B. A. *Biochem. J.* **1992**, *285*, 181−185.

(39) Two additional species with $S = 5/2$ (0.1 spin/$\alpha\beta$) and $S = 9/2$ (0.3 spin/$\alpha\beta$) have been observed for CODH from *M. soehngenii*.[35] These signals appear at potentials above $E^{o\prime} \approx -280$ mV. Jetten *et al*.[35] suggest a possible link of the $S = 9/2$ signal with that attributed to Fe_6S_6 prismane clusters. The $S = 5/2$ signal of *M. soehngenii* is similar to that reported[31] for methylviologen-oxidized $CODH_{Rr}$. We have not observed this signal in any of our recent $CODH_{Rr}$ preparations.

(40) Stephens, P. J.; McKenna, M.-C.; Ensign, S. A.; Bonam, D.; Ludden, P. W. *J. Biol. Chem.* **1989**, *264*, 16347−16350.

(41) Bonam, D.; McKenna, M. C.; Stephens, P. J.; Ludden, P. W. *Proc. Natl. Acad. Sci. U.S.A.* **1988**, *85*, 31−35.

(42) Smith, P. K.; Krohn, R. I.; Hermanson, G. T.; Mallia, A. K.; Gartner, F. H.; Provenzano, M. D.; Fujimoto, E. K.; Goeke, N. M.; Olson, B. J.; Klenk, D. C. *Anal. Biochem.* **1985**, *150*, 76−85.

(43) Lundie, L. L., Jr.; Drake, H. L. *J. Bacteriol.* **1984**, *159*, 700−703.

(44) Ragsdale, S. W.; Wood, H. G. *J. Biol. Chem.* **1985**, *260*, 3970−3977.

(45) Ramer, S. E.; Raybuck, S. A.; Orme-Johnson, W. H.; Walsh, C. T. *Biochemistry* **1989**, *28*, 4675−4680.

(46) Dutton, P. L. *Methods Enzymol.* **1978**, *54*, 411−435.

then passing through 100 mM MOPS, pH 7.3, containing 0.05 mM dithionite and either 5 mM $NiCl_2$ or 5 mM $^{61}NiCl_2$.[28] Excess $NiCl_2$ or $^{61}NiCl_2$ was removed by passing 20 column volumes of 50 mM NaCl and 1 mM EDTA in 100 mM MOPS, pH 7.3, followed by elution of Ni- and ^{61}Ni-activated CODH in 400 mM NaCl/MOPS buffer. Ni- and ^{61}Ni-activated $CODH_{Rr}$ were oxidized by adding indigo carmine (1 mM final concentration), and removing excess oxidant with Sephadex G-25.[30] Indigo carmine-oxidized Ni-deficient $CODH_{Rr}$ was prepared similarly after first removing dithionite.

Preparation of Partially-Reduced $CODH_{Ct}$. A sample of ^{57}Fe-enriched $CODH_{Ct}$ (13 mL of batch 1; 7.2 mg/mL) was applied to a Sephadex G25 column equilibrated in 50 mM Tris, pH 8.0. The resulting dithionite-free sample was concentrated to 2.0 mL using an Amicon cell (W. R. Grace). An aliquot (100 μL) was transferred to a capillary EPR tube and frozen. Another aliquot (550 μL) was mixed with 165 μL of 2.1 mM thionin. Part of this 2.0 equiv/$\alpha\beta$ oxidized sample was transferred to an EPR tube, the remainder to a Mössbauer cup. Both samples were frozen simultaneously within 3 min of adding the thionin. Another aliquot (500 μL) was mixed with 100 μL of thionin, and the resulting 1.3 equiv/$\alpha\beta$ oxidized sample (1 equiv = 1 e^-) was divided up into EPR and Mössbauer tubes as above. The remaining 500 μL was mixed with 52 μL of thionin, and the resulting 0.7 equiv/$\alpha\beta$ oxidized sample was divided as above. The EPR spectra of these samples were compared. The sample oxidized by 0.7 equiv/$\alpha\beta$ thionin exhibited a minor $g = 1.94$ signal and a $g_{av} = 1.82$ signal with about 86% of the intensity of that from the stock solution (after correcting for dilution effects). The samples oxidized by 1.3 and 2.0 equiv/$\alpha\beta$ thionin exhibited the $g_{av} = 1.82$ signal with intensities about 64% and 41%, respectively, of that from the stock (the $g = 1.94$ signal was absent in spectra from both samples).

Preparation of the Fully-Oxidized and CN^--Inhibited $CODH_{Ct}$ Sample. A sample of ^{57}Fe-enriched $CODH_{Ct}$ (batch 2) was concentrated with a Centricon to 500 μL, 122 mg/mL, and then reacted with 126 μL of a 9.4 mM standardized thionin solution. Part of the 5 equiv/$\alpha\beta$ oxidized sample (100 μL) was frozen in an EPR tube, and the remainder was frozen in a Mössbauer cup. After analysis, the sample was mixed with 12 mg of $CODH_{Ct}$ from the same stock solution (affording 73 mg total), and eventually reacted with 55 μL of 10 mM KCN in 50 mM NaOH. The sample had 450 units/mg of CO oxidation activity before, and 12 units/mg after adding CN^-. EPR and Mössbauer samples were prepared and frozen.

Preparation of the Reduced α Subunit. A number of ^{57}Fe-enriched $CODH_{Ct}$ samples (from both batches) were combined and chromatographed through Sephadex G25 equilibrated with 50 mM Tris, pH 8.0. The α subunit was isolated from the resulting solution, as described.[11] The sample was transferred to a Mössbauer cup, oxidized with enough thionin to turn it slightly blue, and then frozen after 5 min. After Mössbauer spectra were collected, the sample was thawed, mixed with dithionite (2 mM final concentration), and refrozen for further Mössbauer studies.

Spectroscopy. Mössbauer spectra were recorded with two spectrometers operating in the constant acceleration mode. One spectrometer allows samples to be studied between 1.5 and 250 K in parallel applied fields up to 8.0 T. The other spectrometer covers the same temperature range but is restricted to applied fields <0.05 T. EPR spectra were recorded with a Bruker ESP 300 spectrometer using an Oxford Instruments ER910A cryostat. EPR spectral simulations were performed using software developed by Dr. M. Hendrich at Carnegie Mellon University.

Results

Carbon monoxide dehydrogenases from various sources appear to contain similar active-site clusters for reversibly oxidizing CO to CO_2. We have uniformly called these sites *C-clusters*, although it has not been established whether they indeed have a common structure and common properties. $CODH_{Rr}$ is the simplest of the CODH's because the enzyme is a monomer and appears to contain only the B- and C-clusters, but not the A-cluster. $CODH_{Rr}$ can also be obtained in an inactive Ni-deficient form that can be activated by adding Ni^{II}.

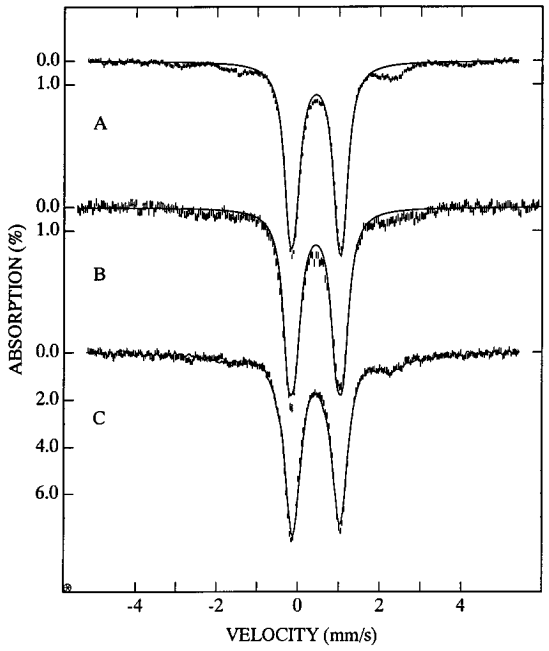

Figure 1. Mössbauer spectra of oxidized CODH samples recorded at 4.2 K in zero magnetic field. (A) Ni-deficient $CODH_{Rr}$, cluster state [B_{ox}:C^*_{ox}]. The solid line, drawn to represent 90% of the absorption, is the result of a least-squares fit to the main doublet with the parameters of Table 2. (B) $CODH_{Rr}$ (batch 1) poised at −15 mV (vs NHE), [B_{ox}:C_{ox}]. The solid line is drawn to represent 90% of the absorption. (C) Comparison of spectra of thionin-oxidized $CODH_{Rr}$ (batch 1) (hash marks), [B_{ox}:C_{ox}], and $CODH_{Ct}$ (solid line), [A_{ox}:B_{ox}:C_{ox}].

Our strategy was to examine $CODH_{Rr}$ in the Ni-deficient and holo forms, in various oxidation states, using the combined Mössbauer/EPR spectroscopic approach.[47] By elucidating the structure of the precursor Fe−S cluster that, upon addition of Ni^{II}, yields the C-cluster, the structure of the C-cluster itself might be determined. Then by comparing spectra of $CODH_{Rr}$ to those from $CODH_{Ct}$, the degree of similarity between the C-clusters in the two enzymes could be evaluated.

Anticipating our results, $CODH_{Rr}$ contains one B-cluster and one C-cluster. The B-cluster is stable in two states (B_{ox} and B_{red}), while the C-cluster is stable in at least three states (C_{ox}, C_{red1}, and C_{red2}); a fourth form of the C-cluster, $C_{S=3/2}$, has electronic spin $S = 3/2$. Ni-deficient $CODH_{Rr}$ does not contain a complete, functional C-cluster (since it lacks Ni), but it does contain an iron−sulfur precursor that will be called the C*-cluster. C* is stable in two states, C^*_{ox} and C^*_{red}. C^*_{red} and $C_{S=3/2}$ may be the same state, but this is uncertain. The cluster states of the proteins will be designated [B_m:X_n], where m = ox or red, X = C or C*, and n = ox, red1, red2, or $S = 3/2$. For $CODH_{Ct}$, which additionally contains the A-cluster, states will be designated [A_l:B_m:C_n], where l = ox or red.

Studies of Fully-Oxidized Ni-Deficient $CODH_{Rr}$, Holo-$CODH_{Rr}$, and $CODH_{Ct}$. The [B_{ox}:C^*_{ox}], [B_{ox}:C_{ox}], and [A_{ox}:B_{ox}:C_{ox}] States. We have studied the Mössbauer spectra of Ni-deficient $CODH_{Rr}$ as well the $CODH_{Rr}$ and $CODH_{Ct}$ holoproteins. Figure 1 shows Mössbauer spectra of all three proteins in the oxidized state. These spectra were recorded at 4.2 K in the absence of an applied field. The spectrum of Ni-deficient $CODH_{Rr}$, shown in Figure 1A, exhibits an intense quadrupole doublet with average $\Delta E_Q \approx 1.19$ mm/s and $\delta = 0.44$ mm/s. The shape of the doublet is quite well represented by assuming two doublets of roughly equal intensity with $\Delta E_Q(1) = 1.36$ mm/s, $\Delta E_Q(2) = 1.02$ mm/s, and $\delta_1 = \delta_2 = 0.44$ mm/s. This

(47) Münck, E. *Methods Enzymol.* **1978**, *54*, 346−379.

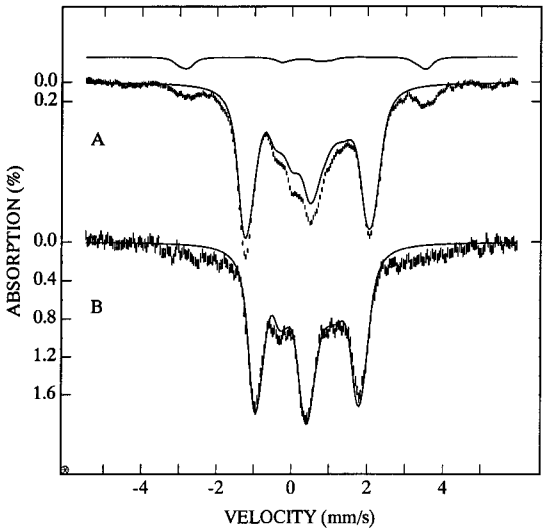

Figure 2. Mössbauer spectra of oxidized CODH recorded at 4.2 K in strong magnetic fields applied parallel to the observed γ-radiation. (A) Ni-deficient $CODH_{Rr}$ at 8.0 T, sample of Figure 1A. The solid line drawn through the data (90% of Fe) is a theoretical curve computed with the parameters of Table 2 with the assumption that all sites are diamagnetic. The solid line drawn *above* the data is a spectral simulation to a component of an $S = 1/2$ minority species (5%) with isotropic magnetic hyperfine interactions. (B) Spectrum (6.0 T) of the sample of Figure 1B. The solid line (90% of the total Fe) is a spectral simulation assuming ΔE_Q and δ values of Table 2 and diamagnetic sites.

representation is, of course, a simplification since the protein contains 7−9 Fe sites; our ability to represent the spectrum by two doublets indicates, however, that the sites are very similar in the oxidized protein. The solid line drawn through the data is a spectral simulation scaled to represent 90% of the total absorption.

Fully oxidized holo-$CODH_{Rr}$ produced nearly identical spectra. The spectrum of Figure 1B was obtained for a sample poised electrochemically at −15 mV; again, the solid line is a simulation representing 90% of the total absorption. In Figure 1C we compare the spectra of thionin-oxidized samples of $CODH_{Rr}$ (hash marks) and $CODH_{Ct}$ (solid line). The two spectra are essentially identical, showing that the oxidized clusters of both enzymes are similar if not identical. Moreover, since $CODH_{Ct}$ contains an additional iron−sulfur cluster, namely, the A-cluster, we can also conclude that the iron−sulfur moiety of the oxidized A-cluster is similar to the oxidized B- and C-clusters.

Figure 2 shows Mössbauer spectra of oxidized samples of Ni-deficient $CODH_{Rr}$ (A) and holo-$CODH_{Rr}$ poised at −15 mV (B), recorded in magnetic fields applied parallel to the observed γ-radiation. The majority component of both spectra reflects Fe sites in diamagnetic environments, as witnessed by the good match of the theoretical spectra (solid lines scaled to 90% of the absorption) with the experimental splittings. The parameters obtained for ΔE_Q and δ, taken together with the observed diamagnetism, are typical for $[Fe_4S_4]^{2+}$ clusters, and they forcefully suggest that all diamagnetic iron components observed here belong to clusters with $[Fe_4S_4]^{2+}$ cores. Thus, Fe_4S_4 cubanes are constituents of the B- and C-clusters of the oxidized holoenzymes. The C*-cluster site of oxidized Ni-deficient $CODH_{Rr}$ contains an $[Fe_4S_4]^{2+}$ cluster as well.

The spectra of all oxidized samples contain broad magnetic components that account for ca. 10% of the total iron in the samples. The broad components absorbing around −3 and +3.5 mm/s velocity do not represent mononuclear Fe^{III} or Fe^{II} sites; the spectral features produced by mononuclear Fe are very

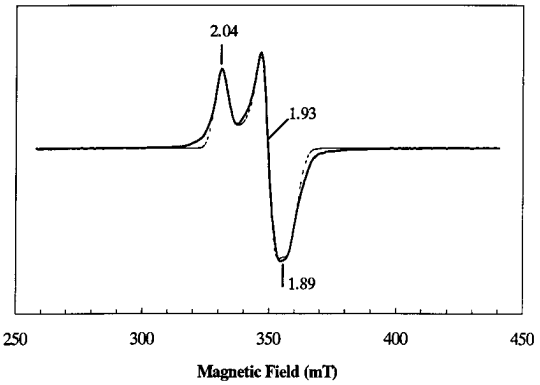

Figure 3. EPR spectrum (10 K) of Ni-deficient $CODH_{Rr}$ reduced with dithionite. The dashed line is a spectral simulation using $g_1 = 2.04$, $g_2 = 1.93$, and $g_3 = 1.89$. EPR conditions: microwave power 1 mW, frequency 9.46 GHz, modulation amplitude 5 G, temperature 10 K.

different from those observed here. In Ni-deficient $CODH_{Rr}$, one of the magnetic components is reasonably well defined, particularly in high-field spectra. The two broad bands at −3 and +3.5 mm/s in Figure 2A are the outer lines of a magnetic component whose splitting increases with increasing applied field, suggesting that it is a subcomponent (ca. 5% of total Fe) of a spin-coupled cluster. The behavior of these bands with increasing field shows that this component belongs to a cluster with spin $S = 1/2$; this component can be simulated with isotropic magnetic hyperfine interactions, $A \approx +30$ MHz (solid line above the data of Figure 2A). EPR spectra of the sample taken after completion of the Mössbauer study revealed a feature with g values at 2.00, 1.99, and 1.93[48] that might be associated with these broad components.

The magnetic components (10% of Fe) observed in the Mössbauer spectra of the oxidized holoenzymes are poorly resolved, suggesting the presence of multiple minority species. The EPR spectra of such samples typically exhibit 2−3 weak signals (each <0.03 spin/mol) around $g = 2$, among them a species with g values ($g_1 \approx 2.14$, $g_2 \approx g_3 \approx 2.03$) reminiscent of the $[Fe_4S_4]^{3+}$ cluster of high-potential iron proteins. A minority species could conceivably be associated with a cluster fragment produced by oxidation at higher potentials. This suggestion is supported for $CODH_{Rr}$ by the observation that samples could not be stabilized at potentials around 0 mV. All samples discussed here were first studied in their reduced states; thus, minority species produced by oxidative damage should not be present in the reduced samples.

Studies of Dithionite-Reduced Ni-Deficient $CODH_{Rr}$. The $[B_{red}:C^*_{red}]$ State. Figures 3 and 4B show EPR spectra of dithionite-reduced Ni-deficient $CODH_{Rr}$ enriched with ^{57}Fe. The $g = 2$ region exhibits a spectrum with g values at 2.04, 1.93, and 1.89; this is the "$g = 1.94$" signal of B_{red}. Under nonsaturating conditions (10 K, 50 μW), the spin concentration

(48) This signal, representing ca. 0.25 spin/mol, has features reminiscent of oxidized Fe_3S_4 clusters. If this interpretation is correct, one-third of the iron atoms of this cluster would be associated with a subsite whose splittings increase with increasing applied field.[48] This tentative interpretation would suggest that ca. 15% of the absorption in Figure 2A belongs to an $[Fe_3S_4]^+$ cluster generated by $Fe_4S_4 \rightarrow Fe_3S_4$ cluster conversion during exposure of the sample to indigo carmine. Such cluster conversions are well documented for aconitase and ferredoxins.[50] If one iron was indeed released from an Fe_4S_4 cluster, the sample should contain some mononuclear iron; indeed, the weak absorption bands at +5 and −4.5 mm/s in the 8.0 T spectrum of Figure 2A indicate the presence of some Fe^{III}.

(49) Kent, T. A.; Huynh, B. H.; Münck, E. *Proc. Natl. Acad. Sci. U.S.A.* **1980**, *77*, 6574−6576.

(50) (a) Kent, T. A.; Emptage, M. H.; Merkle, H.; Kennedy, M. C.; Beinert, H.; Münck, E. *J. Biol. Chem.* **1985**, *260*, 6871−6881. (b) Moura, J. J. G.; Moura, I.; Kent, T. A.; Lipscomb, J. D.; Huynh, B. H.; LeGall, J.; Xavier, A. V.; Münck, E. *J. Biol. Chem.* **1982**, *257*, 6259−6267.

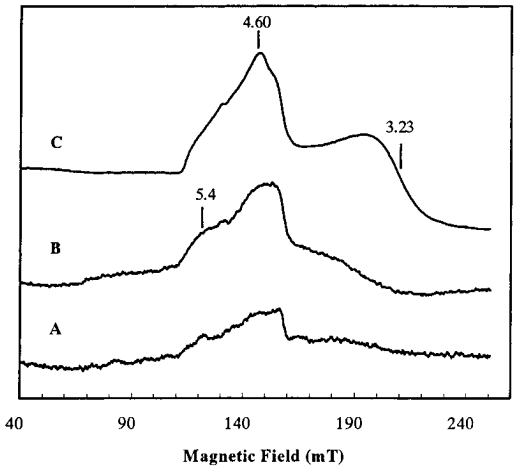

Figure 4. Low-field regions of the EPR spectra of (A) dithionite-reduced samples of $CODH_{Rr}$ (batch 1), temperature 10 K, microwave power 13 mW, frequency 9.46 GHz, modulation amplitude 12 G, (B) Ni-deficient $CODH_{Rr}$, 10 K, 13 mW, 9.46 GHz, 12 G, and (C) the α subunit of $CODH_{Ct}$, 10 K, 20 mW, 9.46 GHz, 12 G. Spectra in (A) and (B) are plotted to reflect the same spectrometer settings and protein concentrations.

of the signal was ∼1 spin/mol, indicating one B-cluster per molecule. Such samples also exhibited signals in the $g = 4-6$ region of the spectrum (Figure 4B). These features are typical of $[Fe_4S_4]^+$ clusters with an $S = 3/2$ ground state, such as that observed for the isolated α subunit of $CODH_{Ct}$ (Figure 4C).[11] The EPR features of $S = 3/2$ $[Fe_4S_4]^+$ clusters are generally broad, a reflection of g strain caused by a distribution of the zero-field splitting parameters D and E about their mean values. Since the signal amplitudes are quite low, the low-field features frequently compete with baseline noise and cavity impurities. For these reasons, the spin concentrations of the $S = 3/2$ signals are difficult to determine with precision, and cluster concentrations are more reliably determined from the Mössbauer data.

Before discussing the Mössbauer data of the reduced sample, it is useful to review the spectral features of $S = 1/2$ and $S = 3/2$ $[Fe_4S_4]^+$ clusters. $S = 1/2$ clusters have Mössbauer patterns that reflect an $Fe^{II}Fe^{III}$ delocalized pair and an $Fe^{II}Fe^{II}$ pair.[51] At temperatures above 100 K, the Mössbauer spectra generally exhibit a pair of nested quadrupole doublets, one from the Fe^{II}-Fe^{II} pair, with $\Delta E_Q \approx 2$ mm/s and $\delta \approx 0.60$ mm/s, and the other from the $Fe^{II}Fe^{III}$ pair, with $\Delta E_Q \approx 1.0-1.4$ mm/s and $\delta \approx 0.53$ mm/s. Thus, one observes a pair of nested doublets as indicated above the data of Figure 5A. In contrast, the four sites of the $S = 3/2$ state yield typically one doublet with $\Delta E_Q \approx 0.8-1.2$ mm/s and $\delta \approx 0.55$ mm/s. In many circumstances, doublets with $\Delta E_Q \leq 1.5$ mm/s are masked by the absorption of other species, while the doublet of the $Fe^{II}Fe^{II}$ pair has larger ΔE_Q values and is generally well resolved. Since the $Fe^{II}Fe^{II}$ pair contributes 50% of the absorption of the $S = 1/2$ cluster, the proportion of iron belonging to such clusters can be readily estimated. In our previous $CODH_{Ct}$ work[12] we have labeled the contribution of the $Fe^{II}Fe^{II}$ pair as ferrous component I (FCI).

At 4.2 K the Mössbauer spectra of the iron sites of protein-bound $[Fe_4S_4]^+$ clusters exhibit magnetic hyperfine interactions described by the tensor **A**, with principal axis components A_j ($j = x, y, z$). The $Fe^{II}Fe^{II}$ pair of the $S = 1/2$ form has a tensor with $A_j > 0$ whereas the $Fe^{II}Fe^{III}$ pair has $A_j < 0$. The magnetic

(51) (a) Middleton, P.; Dickson, D. P. E.; Johnson, C. E.; Rush, J. D. *Eur. J. Biochem.* **1980**, *104*, 289−296. (b) Münck, E.; Papaefthymiou, V.; Surerus, K. K.; Girerd, J.-J. In *Metal Ions in Proteins*; Que, L., Ed.; ACS Symposium Series 372; American Chemical Society: Washington, DC, 1988; Chapter 15, pp 302−325.

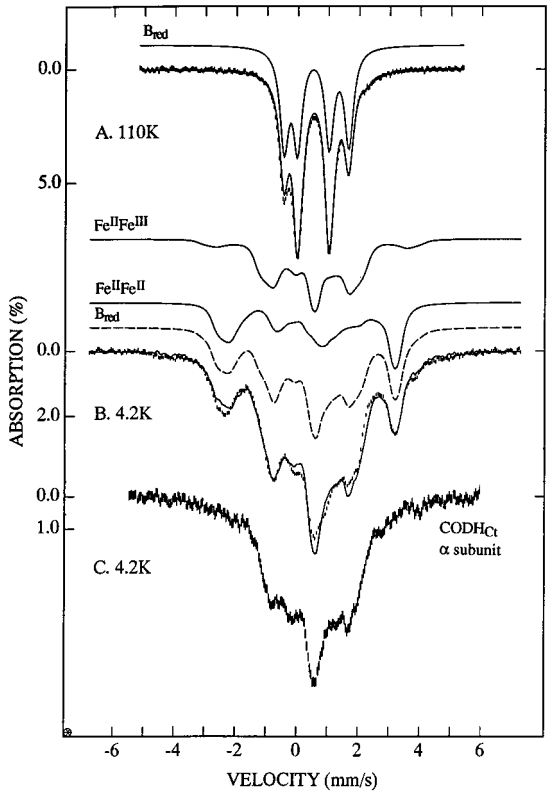

Figure 5. Mössbauer spectra of a dithionite-reduced sample of Ni-deficient $CODH_{Rr}$ (A, B) and α subunit of $CODH_{Ct}$ (C). The lines drawn above the spectra are theoretical curves representing the contributions of the $S = 1/2$ system of B_{red}. Above (A) the nested pair of doublets due to the $Fe^{II}Fe^{III}$ and $Fe^{II}Fe^{II}$ pairs are drawn at 60% of the total absorption; the theoretical curve drawn through the data is a superposition of doublets due to B_{red} (60%) and C^*_{red} (40%). The solid lines above the 6.0 T spectra of (B) are spectral simulations based on eq 1 for the $Fe^{II}Fe^{III}$ and $Fe^{II}Fe^{II}$ pairs of B_{red}; the dashed line gives the total contribution of B_{red}. The solid line drawn through the data of (B) was generated by adding the *experimental* $S = 3/2$ cluster spectrum (40%) of (C) to the *theoretical* spectrum (60%) of B_{red}.

splitting of the $Fe^{II}Fe^{II}$ pair increases with increasing applied field and becomes well resolved in strong applied fields. This is illustrated in Figure 5B where the solid lines drawn above the data show theoretical 6.0 T spectra for both the $Fe^{II}Fe^{II}$ and $Fe^{II}Fe^{III}$ pairs. The magnetic spectra of the four subsites of $S = 3/2$ clusters are generally not resolved. However, all sites have negative A-values. A Mössbauer spectrum of an $S = 3/2$ $[Fe_4S_4]^+$ cluster is shown in Figure 5C.

We have recorded a series of Mössbauer spectra of the dithionite-reduced Ni-deficient $CODH_{Rr}$ between 1.5 and 150 K in applied fields up to 8.0 T. The spectrum obtained at 110 K exhibits two quadrupole doublets. The least-squares fit to the data (Figure 5A, solid line) reveals an outer doublet with $\Delta E_Q = 2.10$ mm/s and $\delta = 0.60$ mm/s. We assign this doublet to the $Fe^{II}Fe^{II}$ pair of B_{red}, the $S = 1/2$ cluster that affords the $g = 1.94$ signal of Figure 3. Since this doublet accounts for 30% of the Fe in the sample, the entire B-cluster should account for 60% of the total Fe. The corresponding $Fe^{II}Fe^{III}$ doublet is not resolved from the remaining innermost doublet, but we estimate its ΔE_Q and δ values to be 1.15 and 0.50 mm/s, respectively. The solid line above the 110 K spectrum is a simulated curve based on the fit representing the two doublets of the B-cluster. The remaining 40% absorption of the original spectrum belongs to a doublet with practically the same parameters as the $Fe^{II}Fe^{III}$ pair of B_{red}, namely, $\Delta E_Q \approx 0.95$ mm/s and $\delta = 0.52$ mm/s. This doublet arises from the C*-

Table 2. Hyperfine Parameters at 4.2 K of Various States in $CODH_{Rr}$

cluster	core oxidation state	spin	number of sites	ΔE_Q (mm/s)	η	δ^a (mm/s)	A_x (MHz)	A_y (MHz)	A_z (MHz)
C^*_{ox}	2+	0	2^b	1.36	0.4	0.44			
			2^b	1.02	1.0	0.44			
C^*_{red}	1+	3/2	2	1.1		0.55			
			2	0.8		0.55			
B_{ox}	2+	0	2^b	1.36	0.4	0.44			
			2^b	1.02	1.0	0.44			
B_{red}	1+	1/2	$Fe^{II}Fe^{II}$	2.10	0.5	0.64	21	26	9
			$Fe^{II}Fe^{III}$	1.15	0.7	0.52	−40	−30	−27
C_{ox}	2+	0	2^b	1.36	0.4	0.44			
			2^b	1.02	1.0	0.44			
C_{red1}	1+	1/2	FCII	2.82	−0.2	0.82	41	18	13
			FCIII	2.35	−0.6	0.62	31	15	7
			$Fe^{II}Fe^{III}$	1.12	0.8	0.53	−30.7	−41	−40

[a] Isomer shifts are quoted relative to Fe metal at 298 K. [b] All oxidized clusters of $CODH_{Rr}$ yield essentially one quadrupole doublet with average $\Delta E_Q = 1.19$ mm/s and $\delta = 0.44$ mm/s. This doublet, to which 8 Fe sites contribute, is analytically well represented by a superposition of two doublets with a width of ~0.32 mm/s for all four lines. The parameters of these two doublets are quoted in Table 2. [c] Because of the isotropic nature of the electronic Zeeman term, the quoted components of the **A** tensors have no spatial correlation to the *g* values. For the simulations of the spectra of the $Fe^{II}Fe^{II}$ pair of B_{red}, the *z* axis of the **A** tensor was rotated by 15° relative to the *z* axis of the electric field gradient tensor.

cluster of Ni-deficient $CODH_{Rr}$, and its parameters are consistent with an $S = 3/2$ $[Fe_4S_4]^+$ cluster.

We have studied the low-temperature Mössbauer spectra in applied fields of 0.05, 2.0, 4.0, 6.0, and 8.0 T. A 6.0 T spectrum recorded at 4.2 K is shown in Figure 5B. By following the magnetic patterns with increasing applied field, the spectra of the $Fe^{II}Fe^{III}$ and $Fe^{II}Fe^{II}$ pairs of B_{red} were readily recognized. The outermost features of the 6.0 T spectrum belong to the ferrous pair. Our spectral simulations indicate that ca. 30% of the total absorption is associated with this component, in excellent agreement with the 110 K data.

We have analyzed the low-temperature spectra of B_{red} with the $S = 1/2$ spin Hamiltonian

$$H = 2\beta \mathbf{S}\cdot\mathbf{H} + \sum_i \{\mathbf{S}\cdot\mathbf{A}_i\cdot\mathbf{I}_i - g_n\beta_n\mathbf{H}\cdot\mathbf{I}_i + (eQV_{zz}(i)/12)[3I_{zi}^2 - 15/4 + \eta(i)(I_{xi}^2 - I_{yi}^2)]\} \quad (1)$$

where **S** is the spin operator of the cluster, $\mathbf{A}_i$ is the magnetic hyperfine tensor of site *i*, and $V_{zz}(i)$ and $\eta(i)$ are the *z*-component and asymmetry parameter of the electric field gradient tensor of site *i*. In eq 1, $i = 1, 2$ sums over the $Fe^{II}Fe^{III}$ and $Fe^{II}Fe^{II}$ pairs. The solid lines above the 6.0 T spectrum of Figure 5B are theoretical curves computed from eq 1 with the parameters listed in Table 2. The dashed line gives the total contribution of B_{red}, normalized to account for 60% of the absorption.

The low-temperature Mössbauer spectra of the C*-cluster are ill-resolved, but they can be identified by similarities with the spectra of the $S = 3/2$ cluster of the $CODH_{Ct}$ α subunit, for which a 6.0 T spectrum is shown in Figure 5C. By normalizing this experimental spectrum to represent 40% of the total Fe and adding the theoretical spectrum of B_{red} at 60% of total Fe, we obtained the solid line drawn through the data of Figure 5B. The quality of the match with the data and the high-temperature Mössbauer spectra (Figure 5A) as well as the EPR spectrum (Figure 4B), taken together, demonstrate that the C*-cluster of Ni-deficient $CODH_{Rr}$ has an Fe_4S_4 core. The cluster is diamagnetic in the oxidized protein and assumes the $S = 3/2$ state in the dithionite-reduced state. The information obtained for the Ni-deficient $CODH_{Rr}$ will enable us to gain substantial insight into the nature of the C-cluster of the $CODH_{Rr}$ and $CODH_{Ct}$ holoproteins. The question of why ca. 60% of the Mössbauer absorption, rather than 50%, is associated with B_{red} arises. A plausible explanation would be to assume that the C-cluster sites have a smaller occupancy than the B-cluster sites; a substoichiometric occupation of the cluster sites is indicated by the finding that the sample had ca. 5.2 Fe atoms/mol of protein.

To summarize, we have presented the following evidence that the C*-cluster is an $[Fe_4S_4]^{1+/2+}$ cluster that has $S = 0$ when oxidized and an $S = 3/2$ ground state in the reduced form. First, C^*_{ox} is diamagnetic and exhibits a quadrupole doublet with parameters typical of $[Fe_4S_4]^{2+}$ clusters. Second, the low-temperature, high-field Mössbauer spectra of C^*_{red} fit those of an $S = 3/2$ $[Fe_4S_4]^+$ cluster. Third, the high-temperature spectrum of C^*_{red} yields a single quadrupole doublet with parameters typical of $S = 3/2$ $[Fe_4S_4]^+$ clusters. Fourth, C^*_{red} exhibits relatively intense EPR features in the $g = 4-6$ range, typical of $S = 3/2$ $[Fe_4S_4]^+$ clusters.

Studies of the $g_{av} = 1.82$ State of Partially-Reduced $CODH_{Rr}$ Holoprotein. As summarized in Table 1, the redox potentials of the B_{ox}/B_{red} couple in $CODH_{Rr}$ is ~−418 mV, while that for the C_{ox}/C_{red1} couple is substantially more positive, namely, −110 mV.[52] These potentials were obtained by fitting plots of the B_{red} (g = 1.94) and C_{red1} ($g_{av} = 1.82$) EPR amplitudes *vs* potential to the $n = 1$ Nernst equation. At potentials below −400 mV, the $g_{av} = 1.82$ signal disappears in a manner not yet well understood and is replaced by the so-called $g_{av} = 1.86$ signal (see below). By setting the potential of samples between these values (e.g., at −300 mV), we expected that essentially all of the molecules would be in a "partially-reduced" state with the B-clusters oxidized and the C-cluster reduced to the C_{red1} state, a state designated $[B_{ox}:C_{red1}]$. We show now that only about 60% of the molecules prepared in this way were actually in that state.

We have set the potential of a ^{57}Fe-enriched sample of holo-$CODH_{Rr}$ to −300 mV and transferred part of the sample into a Mössbauer cuvette and the remainder into an EPR tube.[53] The sample yielded the C_{red1} signal with $g = 2.03$, 1.88, and 1.71,[54] and a minor signal with $g_1 \approx 2.00-2.02$, $g_2 \approx g_3 \approx 1.92$ (Figure 6B). The minor signal and a $g = 2.00$ signal from the benzylviologen mediator are discerned more clearly at 77 K (Figure 6A), since the C_{red1} signal broadens beyond detection at this temperature.[55] In order to quantitate the signal of C_{red1}, we have subtracted from the raw data of Figure 6B a spectral simulation that approximates the shapes of the minor signals of Figure 6A; the result is displayed in Figure 6C. Figure 6D shows an EPR spectrum from a different ^{57}Fe-enriched $CODH_{Rr}$ preparation (batch 2) that lacked the minority species; its $g_{av} = 1.82$ state was attained by oxidation with indigo carmine (see Materials and Methods). Figure 6E shows the $g_{av} = 1.82$ signal

(52) Spangler, N. J.; Ludden, P. W. Unpublished results.

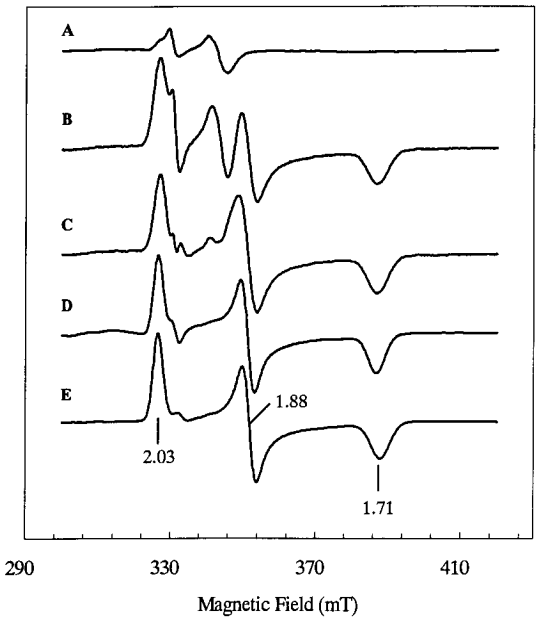

Figure 6. EPR spectra of the [B_{ox}:C_{red1}] state. (A, B) ^{57}Fe-enriched $CODH_{Rr}$ (batch 1) poised at −300 mV; this is the Mössbauer sample of Figures 7 and 8. EPR conditions: (A) temperature 77 K, microwave power 5 mW, frequency 9.24 GHz, modulation amplitude 5 G; (B) 10 K, 1 mW, 9.24 GHz, 5 G. (C) Spectrum obtained by subtracting a spectral simulation for the minority components (∼8% of the total spin concentration) of (A) from the spectrum of (B). (D) Indigo carmine-oxidized sample of batch 2 of ^{57}Fe-enriched $CODH_{Rr}$, 10 K, 20 mW, 9.24 GHz, 12 G. (E) Ni-deficient $CODH_{Rr}$ reconstituted with Ni^{II} and then oxidized with indigo carmine, 10 K, 20 mW, 9.24 GHz, 12 G.

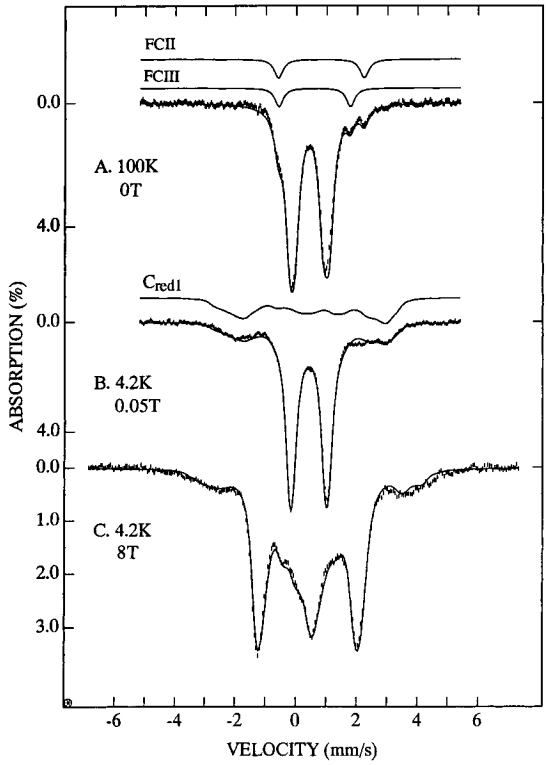

Figure 7. Mössbauer spectra of a 0.27 mM $CODH_{Rr}$ (batch 1) sample poised at −300 mV. The solid line drawn through the 100 K data is a superposition of doublets using the parameters of Table 2, except that all δ values were decreased by 0.02 mm/s to account for second-order Doppler shifts. The contributions of ferrous components FCII and FCIII, each accounting for 7% of the absorption, are drawn separately. The 4.2 K spectra shown in (B) and (C) were simulated as a superposition of diamagnetic species (70% of Fe) and the four paramagnetic subsites (each at 7%) of C_{red1}. For this sample, the cluster contributions to the total absorption are 50% B_{ox}, 30% C_{red1}, and 20% C_{ox}.

of Ni-deficient $CODH_{Rr}$ after reconstitution with ^{61}Ni (same sample as in Figure 11) and treatment with indigo carmine. The similarity of the spectra in Figure 6C−E shows that the Mössbauer sample studied here exhibits a typical $g_{av} = 1.82$ EPR signal.

We have used the following procedure to determine the spin concentration of the ^{57}Fe-enriched sample of Figure 6B. After recording the EPR spectra, the sample was reduced with excess dithionite and immediately frozen for further EPR studies. The resultant spectrum, shown in Figure 12B below, contains the $g = 1.94$ signal of B_{red}. Using computer simulations, we have obtained representations for all spectral components. Comparison of the doubly-integrated simulated spectra of the $g_{av} = 1.82$ and $g = 1.94$ signals yielded the relative spin concentrations $C_{red1}/B_{red} = 0.65$ at 10 K. As shown below, the Mössbauer spectra of the dithionite-reduced sample suggest that the B-cluster is fully reduced. If we assume that the holoenzyme has one B-cluster and one C-cluster, our data suggest that 65% of the C-clusters exhibit the $g_{av} = 1.82$ EPR signal. We have determined the $g_{av} = 1.82$ spin concentration of the samples of Figure 6D,E relative to a Cu·EDTA standard, and obtained ∼0.1 and ∼0.5 spin/mol, respectively.[56]

The 4.2 K Mössbauer spectrum of $CODH_{Rr}$ shown in Figure 7B exhibits two principal spectroscopic components. The quadrupole doublet in the center of the spectrum (70% of Fe) is practically identical to that observed for the oxidized enzyme. It arises from B_{ox} and, as argued below, from a fraction of C-clusters in the C_{ox} (or C^*_{ox}) state. The remainder, accounting for nearly 30% of the total absorption, is a paramagnetic component associated with the $S = 1/2$ system of C_{red1} (the g_{av}

(53) This batch of ^{57}Fe-enriched $CODH_{Rr}$ had high catalytic activity (5090 units/mg). From this batch we were able to produce a Mössbauer sample that yielded a $g_{av} = 1.82$ signal concentration above 0.6 spin/mol; the spectra of this sample are reported in Figures 7 and 8. While this high-activity preparation (batch 1) had the same spectroscopic and redox behavior as other $CODH_{Rr}$ batches, it had an exceptionally high Ni content (ca. 10 Ni atoms/mol). However, none of the Mössbauer components observed for batch 1 had properties different from those of a second ^{57}Fe-enriched preparation (batch 2). While batch 2 had a Ni/Fe ratio of ∼1/8, repeated attempts to produce a Mössbauer sample with $g_{av} = 1.82$ spin concentrations of >0.2 spin/mol failed; we produced, however, from batch 2 an EPR sample having ∼0.5 spin/mol for the $g_{av} = 1.82$ signal. We do not know the cause for the high Ni content of batch 1; its preparation was unusual in that the growth medium was darkly colored (NiS?) and that all purification fractions following cell breakage and DE-52 hydroxylapatite and Sephadex G-25 chromatography were dark gray in color. Batch 2 was made from later cell cultures which did not have the unusual color.

(54) The signal of C_{red1} has $g_{av} = 1.87$. A similar signal, with g values at 2.01, 1.81, and 1.65 ($g_{av} = 1.82$), is observed for $CODH_{Ct}$.[22] Although the signals from both enzymes have slightly different g and g_{av} values, they represent fundamentally the same state. In our $CODH_{Ct}$ studies,[22] we have called C_{red1} the $g_{av} = 1.82$ state. Although g_{av} is different for $CODH_{Rr}$, we will use the nomenclature "$g_{av} = 1.82$". It is frequently more instructive to use the "$g_{av} = 1.82$" rather than the "C_{red1}" nomenclature; thus, we will use both nomenclatures interchangably.

(55) The EPR properties of the minor species with $g_1 \approx 2.0-2.02$, $g_2 \approx g_3 \approx 1.92$ are reminiscent of $[Fe_2S_2]^+$ ferredoxins. If this were the case, the measured spin concentration of ∼0.06 spin/mol would suggest that <2% of the Fe in our sample belongs to this species. The Mössbauer properties of Fe_2S_2 ferredoxins are such that this species would be nearly undetectable in our spectra. The contaminant seen in this particular ^{57}Fe-enriched sample has not been observed in any other $CODH_{Rr}$ preparation. The spin concentration of the minor species is too low for its observation in the spectrum of Figure 12B.

(56) The spectra of Figure 6D,E were recorded at Texas A&M University, while those of Figures 6A,B and 12B were recorded on a Varian V4500 instrument at the University of Wisconsin. At the time of the measurement, a defective switch in the Varian instrument did not allow studies at microwave power below 0.5 mW, preventing spin quantitations relative to a Cu^{II} standard. For this reason, we have chosen the quantitation method described in the text.

= 1.82 species). At 100 K, the electronic spin of C_{red1} relaxes fast on the time scale of Mössbauer spectroscopy as witnessed by the collapse of the magnetic components into quadrupole doublets (Figure 7A). The 100 K Mössbauer spectrum exhibits two doublets, each accounting for 7% of the total Fe, that were not present in the oxidized enzyme. One doublet, labeled Ferrous Component II (FCII), has $\Delta E_Q = 2.82$ mm/s and $\delta =$ 0.80 mm/s. The other, belonging to an Fe site labeled Ferrous Component III (FCIII), has $\Delta E_Q = 2.35$ mm/s and $\delta = 0.60$ mm/s. FCII and FCIII are not present as quadrupole doublets at 4.2 K, showing that they must belong to the C_{red1} paramagnetic component. Thus, they represent two subsites of the C-cluster in the $g_{av} = 1.82$ state. Since C_{red1} contributes ~30% to the total absorption in the 4.2 K spectrum, and FCII and FCIII together account for about half of the C_{red1} absorption (14% of the total Fe), the C-cluster appears to contain two additional subsites. Thus, the C-cluster almost certainly contains a total of four iron subsites (FCII, FCIII, and two others) and is an Fe_4S_4 cluster. If holo-$CODH_{Rr}$ contains the B- and C-clusters in equal proportion, the ~30% Mössbauer absorption associated with C_{red1} suggests that ~60% of the C-clusters exhibit the g_{av} = 1.82 EPR signal, in excellent agreement with 65% obtained from EPR. In what state are the other ~40% of the C-clusters?

To examine this, Mössbauer spectra of the $CODH_{Rr}$ sample poised at −300 mV were obtained in parallel applied fields of 0.05, 2.0, 4.5, and 8.0 T. Given the redox potentials of the B- and C-clusters and the potential at which the sample was poised, we expected that 50% of the absorption of the 8.0 T spectrum (Figure 7C) would reflect diamagnetic species (namely, B_{ox}). However, the central features of the spectrum reflect diamagnetic Fe environments and account for 70% of the absorption. We conclude that the additional 20% of the Fe belongs to the C-clusters in the C_{ox} state (or a state similar to C_{ox} but not reducible at $E^{\circ\prime} = -110$ mV). Thus, 40% of the $CODH_{Rr}$ molecules in the sample appear to be in the [B_{ox}:C_{ox}] state.

We have attempted to identify the two additional subsites in the C_{red1} form of the C-cluster, by subtracting the doublet of the oxidized enzyme (70% of the total Fe), FCII (7%), and FCIII (7%) from the 100 K Mössbauer data. The remaining 16% of the spectral absorption is a doublet with $\Delta E_Q \approx 1.12$ mm/s and $\delta \approx 0.53$ mm/s. The value of δ is very similar to that observed for the $Fe^{II}Fe^{III}$ pair of $[Fe_4S_4]^+$ clusters such as B_{red}, suggesting that this doublet reflects a similar pair in C_{red1}. FCIII, in contrast, has parameters similar to those observed for the two ferrous sites of $[Fe_4S_4]^+$ clusters. The distinctive site of the C-cluster, FCII, has $\delta = 0.82$ mm/s. This value is substantially larger than that of the ferrous sites of $[Fe_4S_4]^+$ clusters coordinated by four cysteinyl ligands. The parameters of FCII remind us of the pentacoordinated Fe_4S_4 cluster site of a synthetic complex reported by R. H. Holm and co-workers.[58] This complex has one site with FeS_3N_2 coordination (see below) with $\Delta E_Q = 2.35$ mm/s and $\delta = 0.83$ mm/s. The comparison with the synthetic complex suggests that FCII is a pentacoordinate site, rather than a tetrahedral site as suggested earlier.[57]

The contribution of C_{red1} to the high-field Mössbauer spectra of the partially-reduced sample of $CODH_{Rr}$ was revealed by subtracting the contributions of B_{ox} and C_{ox} (Figure 8). The magnetic splittings of two subsites of C_{red1} increased with increasing field, while those of the other two subsites decreased. The former sites must belong to FCII and FCIII while the latter are associated with the $Fe^{II}Fe^{III}$ pair; no other assignments produced acceptable fits. Using the $S = 1/2$ Hamiltonian of eq 1, we have obtained, by extensive computer simulations, reasonable fits for the entire data set. These fits are plotted as solid lines drawn through the spectra of Figures 7 and 8; the parameters used are listed in Table 2. Above the spectrum of Figure 8D we have plotted the contributions of FCII and FCIII (summed) and the $Fe^{II}Fe^{III}$ pair. Although the parameters used have substantial uncertainties, the satisfactory fits to the data attest to their overall validity, and they strongly support the notion that C_{red1} has an $[Fe_4S_4]^+$ core that contains one unique site, namely, FCII.

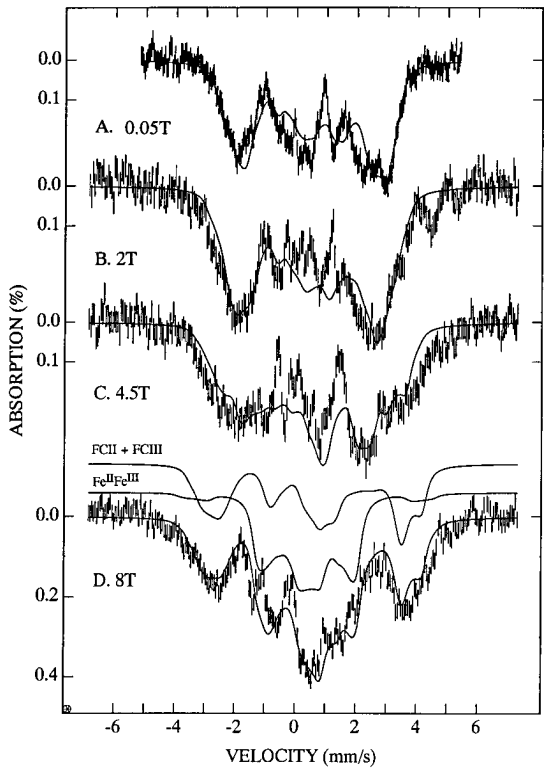

Figure 8. Mössbauer spectra (4.2 K) of C_{red1} taken in applied fields as indicated, same sample as for Figure 7. Spectra were prepared by removing 70% of the (computer-simulated) absorption due to diamagnetic B_{ox} and C_{ox} from the raw data. The solid lines are theoretical curves generated from eq 1 using the parameters listed in Table 2. The solid lines drawn above the 8.0 T data indicate the contributions of FCII, FCIII, and the $Fe^{II}Fe^{III}$ pair.

Studies of Partially-Reduced $CODH_{Ct}$. The [A_{ox}:B_{ox}:C_{red1}] State. During the past four years we have studied many preparations of $CODH_{Ct}$ with EPR and Mössbauer spectroscopy, with particular focus on understanding the nature of the $g_{av} =$ 1.82 state. Using thionin, we have performed oxidative titrations in the −400 to +100 mV range with the goal of correlating the C_{red1} ($g_{av} = 1.82$) EPR signal with the respective Mössbauer components and succeeded in identifying four subsites of the C-cluster by Mössbauer spectroscopy. However, because of the ever-present broad magnetic feature of Figure 1C (~10% of the total Fe), we could not exclude the possibility that the C-cluster had more than four iron sites. In particular, we were unable to decide whether this broad magnetic feature was already present at potentials between −400 and −200 mV where the enzyme exhibited the $g_{av} = 1.82$ signal. For $CODH_{Rr}$, we are reasonably sure that the broad feature was not present in

(57) Previously, we have reported for FCII the values $\Delta E_Q = 2.90$ mm/s and $\delta = 0.70$ mm/s. The value quoted for δ suggested an Fe^{II} site with a tetrahedral sulfur coordination. Our subsequent studies provided much better information for the low-energy line of the FCII doublet, yielding $\Delta E_Q =$ 2.82 mm/s and $\delta = 0.82$ mm/s for both enzymes. The new value for δ suggests a pentacoordinate site (see ref 58 and Discussion).

(58) Ciurli, S.; Carrié, M.; Weigel, J. A.; Carney, M. J.; Stack, T. D. P.; Papaefthymiou, G. C.; Holm, R. H. *J. Am. Chem. Soc.* **1990**, *112*, 2654−2664.

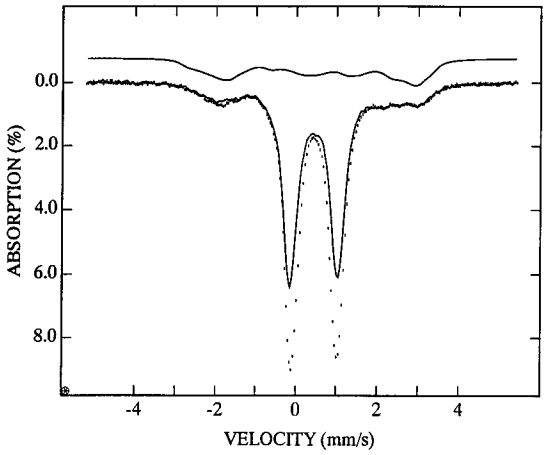

Figure 9. Mössbauer spectra (4.2 K) of $CODH_{Rr}$ (solid line, batch 1) and $CODH_{Ct}$ (hash marks) prepared in states that yield the $g_{av} = 1.82$ signal. The cluster states are [B_{ox}:C_{red1}] and [A_{ox}:B_{ox}:C_{red1}], respectively. Spectra were recorded in a parallel applied field of 0.05 T and are plotted such that the magnetic components of C_{red1} match in amplitude. For illustration, the theoretical spectrum of C_{red1} of $CODH_{Rr}$ is drawn above the data.

the −300 mV sample because all magnetic components observed at 4.2 K are accounted for by the $g_{av} = 1.82$ form of the C-cluster.

A sample of $CODH_{Ct}$ was prepared in the partially-reduced state ([A_{ox}:B_{ox}:C_{red1}]) by removing dithionite and adding 1.3 equiv/$\alpha\beta$ thionin. This sample exhibited the C_{red1} signal and weak (<0.05 spin/$\alpha\beta$) contaminants. The corresponding 4.2 K Mössbauer spectrum exhibits a major quadrupole doublet (∼80% of the total Fe) and a paramagnetic component (∼20% of the total Fe) (Figure 9, hash marks). The doublet is due to A_{ox} and B_{ox} while some or all of the magnetic component is due to C_{red1}. We have shown above that the magnetic component of the equivalent spectrum of $CODH_{Rr}$ (poised at −300 mV, Figure 7B, ∼30% of the total Fe) was due entirely to C_{red1}. The solid line in Figure 9 is this spectrum of $CODH_{Rr}$, scaled to produce the best overlap with the magnetic contributions of the $CODH_{Ct}$ spectrum. The C_{red1} contribution from $CODH_{Rr}$ is also indicated separately by redrawing the theoretical curve of Figure 7B. The magnetic components of the two samples ($CODH_{Rr}$ and $CODH_{Ct}$) overlap almost exactly, indicating that essentially all of the magnetic components of $CODH_{Ct}$ originate from the C_{red1} state of the C-cluster, and that the C-clusters in $CODH_{Rr}$ and $CODH_{Ct}$ have very similar if not identical structures.

Figure 10A shows a 100 K spectrum of the $CODH_{Ct}$ sample of Figure 9. It can be seen that the absorption pattern is very similar to that displayed by the $CODH_{Rr}$ sample of Figure 7A. The absorption of FCII, accounting for 5.5% of the total absorption and outlined above the data, is clearly discernible. The values for $\Delta E_Q = 2.82$ mm/s and $\delta = 0.82$ mm/s are identical to those of $CODH_{Rr}$.[57] Moreover, ΔE_Q is independent of temperature. The spectrum also contains ferrous component III with parameters similar to those of the $CODH_{Rr}$, although its line width is larger than that observed for $CODH_{Rr}$ (the broader lines could reflect heterogeneities and/or relaxation). For $CODH_{Ct}$, we have conducted titration studies, using thionin as an oxidant. These studies have shown that the intensity of FCII correlates with the intensity of the $g_{av} = 1.82$ signal during the early and middle phases of the titration. Because of the ever-present broad magnetic components shown in Figures 1 and 2, we could not follow this correlation for states where the $g_{av} = 1.82$ signal had nearly disappeared.

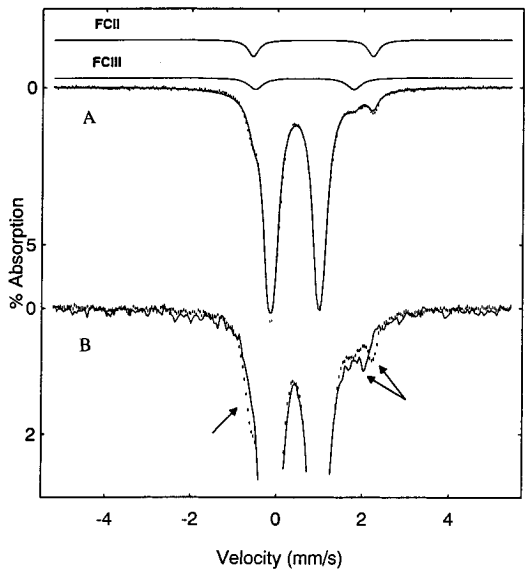

Figure 10. Mössbauer spectra (100 K) of $CODH_{Ct}$ and of $CODH_{Ct}$ added with CN^-. (A) Spectrum of $CODH_{Rr}$ prepared by oxidation with 1.3 equiv of thionin to maximize $g_{av} = 1.82$ state (same sample as in Figure 9). Contributions of spectral components FCII and FCIII are indicated separately. The solid line is a least-squares fit to the spectrum. (B) Comparison of spectra of samples prepared without (hash marks) and with (solid line) CN^-. Features of the central doublet are truncated to emphasize shifts of the lines of FCII upon CN^- binding (arrows).

The inhibitor CN^- binds to the C-cluster in the C_{red1} state and shifts the $g_{av} = 1.82$ signal to one with $g_{av} = 1.72$ (g values at 1.87, 1.78, and 1.55).[18] We have studied the binding of CN^- with Mössbauer spectroscopy by comparing the spectra of partially-reduced $CODH_{Ct}$ samples prepared with and without CN^- (Figure 10 B). It can be seen that the addition of CN^- leads to a decrease of the quadrupole splitting of FCII; at 100 K, ΔE_Q of FCII changes from 2.82 to 2.52 mm/s. This change is quite substantial, and it suggests that CN^- binds to FCII. The isomer shift of FCII is the same in both states, showing that FCII retains its ferrous character. Moreover, the notion that FCII may represent the CN^- binding site is not unreasonable since, as we argued above, it represents a site of an Fe_4S_4 cluster with special coordination. The spectra of the CN^- adduct are not well resolved, and we could thus not establish whether the other iron sites of the cluster were affected by the addition of the inhibitor.

An earlier study of $CODH_{Rr}$ indicated that the $g = 2.03$ feature of C_{red1} broadened by about 8 G and shifted by 4 G when the protein was labeled with ^{61}Ni.[40] We have repeated these experiments by incubating Ni-deficient enzyme with ^{61}Ni and oxidizing the resulting holo-$CODH_{Rr}$ with indigo carmine to produce a strong $g_{av} = 1.82$ signal. EPR spectra with and without ^{61}Ni enrichment are shown in Figure 11. A detailed comparison of the line shapes of the two $CODH_{Rr}$ samples shows that the widths of the $g = 1.88$ and 1.71 resonances match within 1 G; the $g = 2.03$ resonance shows a 2 G broadening and a 1 G shift for the ^{61}Ni-enriched sample. For $CODH_{Ct}$, the $g = 2.01$ and 1.65 resonances of the enriched and unenriched samples have the same width to within 1 G. The $g = 1.82$ derivative feature of the ^{61}Ni-enriched $CODH_{Ct}$ sample was distorted by the presence of a minor contaminant; however, the central part and the high-field portion of the feature showed no effects of the ^{61}Ni. In order to check the reproducibility, we have compared $CODH_{Rr}$ samples from four different batches containing Ni in natural abundance. The $g = 2.03$ resonances of holo-$CODH_{Rr}$ of two recent batches had 27 and

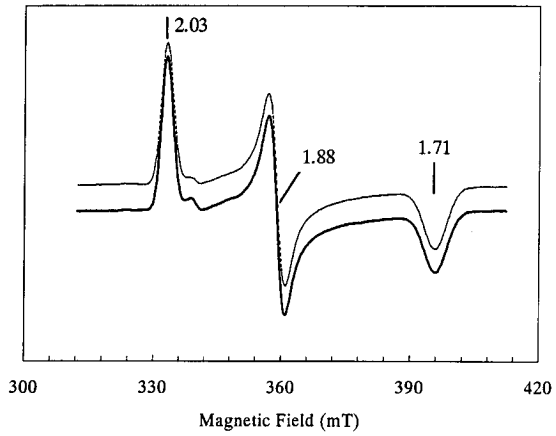

Figure 11. EPR spectra of the C_{red1} state of $CODH_{Rr}$ prepared by reconstitution of Ni-deficient protein with Ni in natural abundance (lower trace) and ^{61}Ni enriched to 90% (upper trace). EPR conditions: temperature 10 K, microwave power 20 mW, frequency 9.46 GHz, modulation amplitude 12 G.

28 G widths, while those of the Ni-reconstituted protein were 36 G for the sample of Stephens *et al.*[40] and 32 G for our sample of Figure 11. Thus, the 2 G broadening observed for the ^{61}Ni sample seems to fall within the variations observed in spectra from different preparations. A variability in line width may also explain the 8 G broadening observed previously.[40]

Studies of Fully-Reduced $CODH_{Rr}$. The $[B_{red}:C_{red2}:C_{S=3/2}]$ State. The spectral similarity of the C-clusters of $CODH_{Rr}$ and $CODH_{Ct}$ in the states C_{ox} and C_{red1} is remarkable, strongly suggesting a common structure of the C-cluster. However, the C_{red2} state of the C-cluster in $CODH_{Rr}$ had not been reported, and we wondered whether the common properties of the C-clusters included formation of C_{red2} states.

To examine this, $CODH_{Rr}$ was reduced with CO and immediately frozen for EPR analysis. The spectrum (Figure 12A) exhibits the $g = 1.94$ signal from B_{red} ($g = 2.04$, 1.93, 1.88), a remnant of the $g_{av} = 1.82$ signal, and a new signal with $g_{av} = 1.86$ ($g = 1.97$, 1.87, 1.75). Spin quantitation of the signals yielded relative concentrations of 1.0, 0.5, and 0.15 for the $g = 1.94$ signal, the $g_{av} = 1.86$ species, and the remnant $g_{av} = 1.82$ species, respectively. Given the similar g values for the $g_{av} = 1.86$ signal from $CODH_{Rr}$ and the $g_{av} = 1.86$ signal from $CODH_{Ct}$ and the similar method of preparing the two states, we conclude that they both reflect the same C_{red2} state. We have observed the $g_{av} = 1.86$ signal also when $CODH_{Rr}$ was reduced with dithionite. The EPR spectra of a sample from the ^{57}Fe-enriched enzyme (see Figures 12B and 4A) reveal that the dithionite-reduced enzyme exhibits the same g values for C_{red2} as the CO-reduced sample. The intensity of the $g_{av} = 1.82$ signal is very weak for the dithionite-reduced sample. Both the CO- and dithionite-reduced $CODH_{Rr}$ samples exhibit resonances in the $g = 4-6$ region of the spectra, showing that some C-clusters have $S = 3/2$ (designated as $C_{S=3/2}$). The low-field regions of the EPR spectra of the dithionite-reduced samples of holo-$CODH_{Rr}$ and Ni-deficient $CODH_{Rr}$, shown in Figure 4A,B, are normalized to the same protein concentration, microwave power, and receiver gain, and relative intensities may be compared directly. The intensity of the low-field features in reduced holo-$CODH_{Rr}$ is about half that in Ni-deficient $CODH_{Rr}$. Since all of the C*-clusters of Ni-deficient $CODH_{Rr}$ are $S = 3/2$ $[Fe_4S_4]^+$ clusters, a comparison of the intensities suggests that roughly half of the C-clusters in populations of holo-$CODH_{Rr}$ are in the $C_{S=3/2}$ state.[59] The presence of a

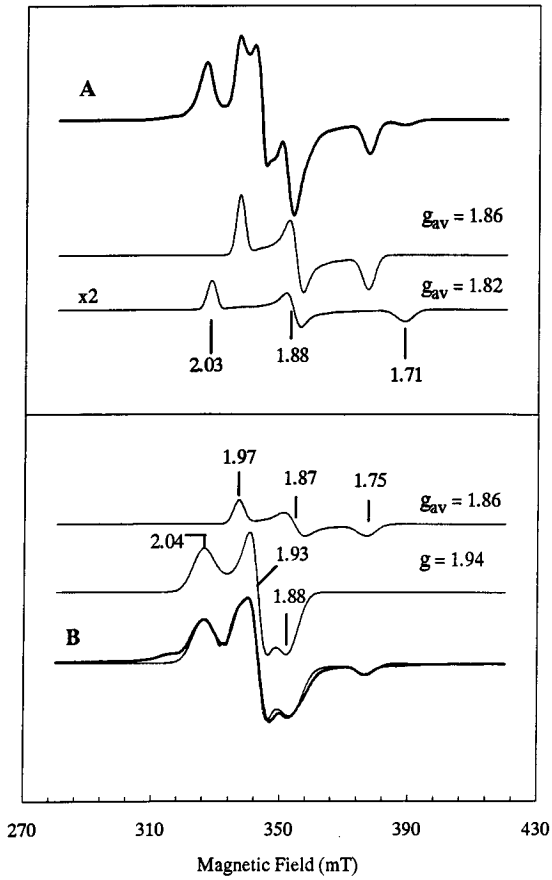

Figure 12. EPR spectra of $CODH_{Rr}$ (batch 2) reduced either with CO (A) or with dithionite (B). (A) Spectrum (10 K) of $CODH_{Rr}$ reduced with CO. The solid lines below the experimental spectrum of (A) are spectral simulations for the $g_{av} = 1.82$ and $g_{av} = 1.86$ species. In order to achieve strong signals for the $g_{av} = 1.86$ and 1.82 species, the microwave power was set at 20 mW. Under these conditions the $g = 1.94$ signal of B_{red} is slightly saturated; for quantitative analysis, we have used spectra recorded at 50 μW power. The relative spin concentrations of the $g = 1.94$, $g_{av} = 1.86$, and $g_{av} = 1.82$ species were 1, 0.5, and 0.15, respectively. EPR conditions: temperature 10 K, microwave power 20 mW, frequency 9.46 GHz, modulation amplitude 12 G. (B) Spectrum (10 K) of ^{57}Fe-enriched $CODH_{Rr}$ reduced with dithionite; the low-field region of this sample is shown in Figure 4A. Spectral simulations of the $g = 1.94$ and $g_{av} = 1.86$ species are shown above the data. EPR conditions: temperature 10 K, microwave power 50 μW, frequency 9.46 GHz, modulation amplitude 11.8 G.

C-cluster having $S = 3/2$ in fully-reduced $CODH_{Rr}$ is further supported by the Mössbauer data.

We have studied one sample of dithionite-reduced $CODH_{Rr}$ with Mössbauer spectroscopy. Since the spectra are exceedingly complex, we will only describe their principal features. The 4.2 K data had features typical of systems with weakly interacting spins, as witnessed by the observation that in fields of 0.01, 0.05, and 0.3 T the shapes of the Mössbauer spectra changed with the field. This behavior can be attributed to spin−spin interactions between the C- and B-clusters within the same molecule. An applied field of 0.5 T was required to decouple these interactions, suggesting that the clusters are separated by

(59) We do not yet have much experience with preparing the fully reduced states of $CODH_{Rr}$. We have noticed that dithionite-reduced samples have to be frozen within 1−2 min after reduction, if the C_{red2} state is to be attained. Samples of reduced $CODH_{Rr}$ slowly oxidize even when kept under anaerobic conditions. Some of these observations were made in the later phase of the studies reported here, and one should not be surprised if subsequent EPR and Mössbauer studies of dithionite-reduced $CODH_{Rr}$ yield somewhat different proportions for the various species. These matters are currently under study.

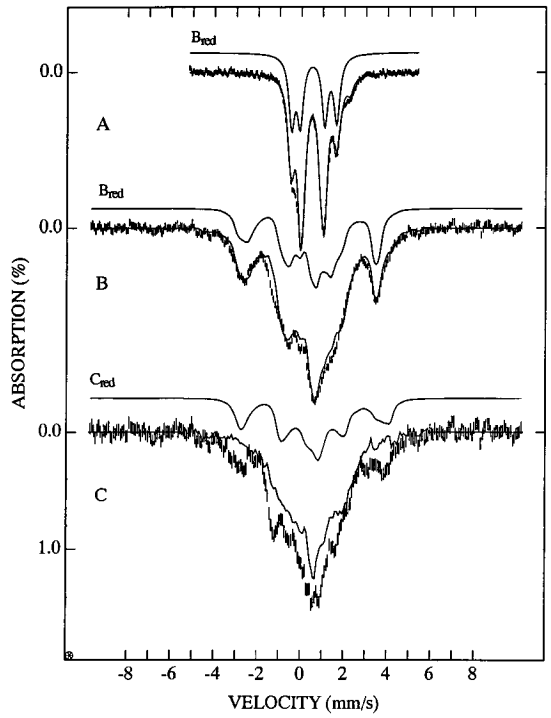

Figure 13. Mössbauer spectra of dithionite-reduced $CODH_{Rr}$ (batch 1). (A) Spectrum recorded at 110 K. The solid line is a least-squares fit to the data. The contribution of B_{red} is shown separately above the experimental spectrum. (B) Spectrum recorded at 4.2 K in a parallel field of 8.0 T. Drawn above the data is the theoretical spectrum of B_{red}. (C) Spectrum (8.0 T) obtained by subtracting the theoretical spectrum (45% of the total area) of B_{red} from the raw data of (B). The solid line drawn above spectrum C is the theoretical spectrum of C_{red1}. For comparison we have also plotted the experimental 8.0 T spectrum (jagged solid line) of the α subunit of $CODH_{Ct}$.

≤15 Å. We have observed similar interactions for the Ni-deficient $CODH_{Rr}$ sample of Figure 5.

Since the EPR spectra of dithionite-reduced $CODH_{Rr}$ exhibit signals from at least three species, namely, B_{red}, C_{red2}, and $C_{S=3/2}$, the corresponding 4.2 K Mössbauer spectra are superpositions of at least 12 magnetic subspectra of unknown proportions. Moreover, the low-field spectra are affected by intramolecular spin−spin interactions. For these reasons, our analysis is limited, though some spectral features are readily recognized. The rightmost line in the spectrum of Figure 13A belongs to a quadrupole doublet (∼5% of the total Fe) that has apparently the same parameters as component FCII of the C_{red1} state. This suggests that an FCII-type component is also present in the C_{red2} state. The spectra also exhibit doublet FCI of B_{red}. The Mössbauer spectra of B_{red} in holo-$CODH_{Rr}$ appear to be identical to those observed for reduced Ni-deficient $CODH_{Rr}$. We estimate that ∼45% of the absorption in the spectra of Figure 13 belongs to B_{red}; these contributions are drawn separately above the raw data. For further analysis, we refer to Figure 13C which shows an 8.0 T spectrum obtained by removing the theoretical spectrum of B_{red} from the raw data of Figure 13B. The shape of the spectrum of Figure 13C is very similar to that observed for the $S = 3/2$ $[Fe_4S_4]^+$ cluster of the α subunit of $CODH_{Ct}$; for comparison, the spectrum of the α subunit is also shown in Figure 13C. The similarity of the spectra, together with the observation of $S = 3/2$ resonances in the $g = 4-6$ region of the EPR spectra, strongly suggests that dithionite-reduced $CODH_{Rr}$ harbors a fraction of molecules containing an $S = 3/2$ $[Fe_4S_4]^+$ cluster; this state is designated as $C_{S=3/2}$.

The EPR spectra of dithionite-reduced $CODH_{Rr}$ exhibit the $g_{av} = 1.86$ signal of C_{red2}. Therefore, the low-temperature Mössbauer spectra must contain another magnetic component. Since the 100 K Mössbauer spectrum of fully-reduced $CODH_{Rr}$ contains a doublet representing ∼5% of the iron similar to, or identical with, FCII of the C_{red1} state, we may anticipate that 20% of the low-temperature absorption belongs to the C_{red2} form of the C-cluster. The difference spectrum of Figure 13C has absorption features around −3 and +4 mm/s which do not belong to $C_{S=3/2}$ or B_{red}. Above the data of Figure 13C we have drawn the theoretical spectrum of C_{red1} (same curve as shown in Figure 8D). It can be seen that the outermost features of the theoretical C_{red1} spectrum match the experimental features reasonably well, suggesting that the Mössbauer spectrum of C_{red2} is quite similar to that of C_{red1}. We have obtained a reasonable representation of the experimental spectrum of Figure 13B by summing the theoretical spectra for the B-cluster (45%), the C_{red2} state of the C-cluster (20%), and the $S = 3/2$ cluster of the α subunit of $CODH_{Rr}$ (35%); this sum is the solid line drawn through the data of Figure 13B. We do not suggest that we have a valid representation for C_{red2}. However, we believe that roughly 25−35% of the absorption of our sample is attributable to an $S = 3/2$ $[Fe_4S_4]^+$ cluster. This suggests that 50−70% of the C-clusters are in the $C_{S=3/2}$ state while ca. 40% are in the C_{red2} state. Our analysis leaves little doubt that the C-clusters of $CODH_{Rr}$ occur in different forms, and the present study has identified which forms need to be considered.

Discussion

Formation and Structure of the C-Cluster. Our results demonstrate that Ni-deficient $CODH_{Rr}$, a catalytically inactive form of $CODH_{Rr}$ that can be activated by adding Ni, contains two $[Fe_4S_4]^{1+/2+}$ clusters. When reduced, one of these clusters exhibits a $g = 1.94$ EPR signal and a distinctive quadrupole doublet (FCI) arising from its $Fe^{II}Fe^{II}$ pair. These EPR and Mössbauer features, including the hyperfine parameters listed in Table 2, are typical of $[Fe_4S_4]^{1+/2+}$ clusters coordinated to four cysteinyl ligands. We call this cluster the *B-cluster* because these characteristics are the same as those of the B-cluster in $CODH_{Ct}$. Holo-$CODH_{Rr}$ also contains an $[Fe_4S_4]^{1+/2+}$ cluster with properties virtually identical to those of the B-cluster of $CODH_{Ct}$.

The other $[Fe_4S_4]^{1+/2+}$ cluster in Ni-deficient $CODH_{Rr}$ is the precursor for the C-cluster in holo-$CODH_{Rr}$. This cluster, called the *C*-cluster*, is diamagnetic when oxidized, and has cluster spin $S = 3/2$ when reduced. The reduced C*-cluster exhibits EPR signals in the range $g = 6-3$ and Mössbauer features typical of other $S = 3/2$ clusters[11,60,61] (e.g., the $S = 3/2$ $[Fe_4S_4]^+$ cluster from the α subunit of $CODH_{Ct}$). It does not exhibit the FCII or FCIII subsite, or the $g_{av} = 1.82$ or 1.86 signals typical of the C-cluster of holo-CODH. Moreover, CN^- does not appear to bind to the C*-cluster.[28] All known properties of the C*-cluster suggest a standard $[Fe_4S_4]^{1+/2+}$ cluster, with tetrahedral coordination at each Fe site. While cysteinyl residues are the likely coordinating residues, we cannot rule out the possibility that one Fe site has a ligand such as the aspartate observed for the $S = 3/2$ form of *Pyrococcus furiosus* ferredoxin.[61]

When Ni^{II} is incorporated into Ni-deficient $CODH_{Rr}$, the C*-cluster is converted into the C-cluster. The Mössbauer data obtained for the C-cluster indicate four iron subsites, including

(60) (a) Lindahl, P. A.; Day, E. P.; Kent, T. A.; Orme-Johnson, W. H.; Münck, E. *J. Biol. Chem.* **1985**, *260*, 11160−11173. (b) Carney, M. J.; Papaefthymiou, G. C.; Spartalian, K.; Frankel, R. B.; Holm, R. H. *J. Am. Chem. Soc.* **1988**, *110*, 6084−6095.

(61) Srivastava, K. K. P.; Surerus, K. K.; Conover, R. C.; Johnson, M. K.; Park, J.-B.; Adams, M. W. W.; Münck, E. *Inorg. Chem.* **1993**, *32*, 927−936.

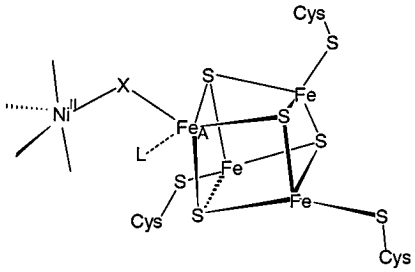

Figure 14. Illustration of the C-cluster model discussed in the text. Fe_A is drawn bridged to the Ni. We have drawn this site as if it were pentacoordinate site FCII. We would find this arrangement aesthetically appealing, but caution the reader that neither our data nor the coupling model excludes the possibility that an Fe atom other than FCII may, in fact, be bridging. Moreover, we have assumed that the nonbridging iron atoms of the cluster are coordinated by cysteinyl ligands, but this very common arrangement is also not required.

the distinctive FCII subsite. The less distinct sites have the Mössbauer properties of an $Fe^{II}Fe^{III}$ delocalized pair of an $[Fe_4S_4]^+$ cluster, while FCII and FCIII are ferrous sites. Thus, the conversion from the precursor C*-cluster to the C-cluster does *not* involve a change in the Fe_4S_4 core structure. However, the coordination environment of one of the irons of the cluster (FCII) changes substantially by incorporation of the Ni into the protein. The properties of FCII suggest a pentacoordinated subsite of the $[Fe_4S_4]^+$ cluster. A cluster site with nontetrahedral coordination was first demonstrated by Mössbauer spectroscopy for Fe_a, the substrate binding site of the Fe_4S_4 cluster in aconitase with unique hexacoordinate geometry.[62] Extensive ENDOR[63a] and X-ray studies[63b] have further characterized Fe_a. The aconitase results prompted a systematic study in R. H. Holm's laboratory to create site-specific modifications at one subsite of an Fe_4S_4 cluster. This group synthesized a cube with a pentacoordinated FeS_3N_2 site by substituting the standard thiolate with a pyrazolyl borate ligand.[58] The pentacoordinated site of the synthetic complex has the same isomer shift as FCII, but a slightly smaller ΔE_Q ($\delta = 0.83$ mm/s and $\Delta E_Q = 2.38$ mm/s at 4.2 K). The special nature of the FCII site is also indicated by our observation that the quadrupole splitting of the FCII site of $CODH_{Ct}$ changes from 2.82 to 2.55 mm/s upon addition of CN^-.

How the coordination of the FCII subsite increases when Ni is incorporated into Ni-deficient $CODH_{Rr}$ is uncertain. It is conceivable that the Ni competes for a ligand of the C*-cluster and that this ligand is removed from the cluster, creating an open site to which another protein residue and, perhaps, a water (hydroxide) ligand can coordinate. Alternatively, the Ni and the FCII site may share a ligand. Accordingly, the Ni would be linked to the FCII iron of the cluster via a bridging ligand X, as shown in Figure 14. We have assumed a distorted pentacoordinate geometry with 3 N/O atoms and 2 S donors for the Ni center, as concluded from XAS studies.[27] However, our data cannot exclude the possibility that the Ni is located further from the cluster, and that it affects FCII indirectly via a conformational change of the protein.

The substantial shift observed for ΔE_Q of FCII when CN^- is added to $CODH_{Ct}$ suggests that CN^- binds to FCII. Since CN^- does not appear to bind to the C*-cluster in Ni-deficient $CODH_{Rr}$, the presence of the Ni and/or the increased coordination of FCII caused by Ni binding appears to activate FCII for binding the inhibitor CN^-. Ni binding also activates this site for catalysis. The substrate CO does not reduce the Fe−S cluster of Ni-deficient $CODH_{Rr}$, suggesting that the C*-cluster is unable to accept electrons from CO. Thus, it appears that the Ni and FCII iron are together intimately involved in CO oxidation catalysis, and we suspect that CO oxidation/CO_2 reduction catalysis occurs at the [Ni:FCII] heterobimetallic site of the C-cluster. For example, a water or hydroxyl may bind to FCII and CO/CO_2 may bind the Ni. For CO oxidation, the OH^- bound to FCII could be strategically positioned for nucleophilic attack on the carbonyl carbon.

Electronic Structure of C_{red1}. The C_{red1} state of the C-cluster from $CODH_{Rr}$ appears to have electronic properties similar to that of reduced, activated aconitase. The clusters of both enzymes are of the $[Fe_4S_4]^+$ type, with one distinct penta- to hexacoordinate site. Both have $S = 1/2$ spin states and exhibit similar EPR signals. With *trans*-aconitate bound, the aconitase cluster has a signal with g values of 2.01, 1.875, and 1.796,[64] while the C_{red1} state of the C-cluster exhibits a signal with g values of 2.03, 1.88, and 1.71. Moreover, all reported $[Fe_4S_4]^+$ clusters have their highest g value between $g = 2.04$ and $g = 2.09$[65] except the C-cluster and aconitase with *trans*-aconitate bound. Thus, it is possible that the electronic state of C_{red1} is essentially the same as that of the $[Fe_4S_4]^{2+/1+}$ cluster of active aconitase with substrate/inhibitor bound (however, we prefer a pentacoordinate FCII site). In this picture, the Ni would be electronically isolated from the cluster, and since the Ni is also EPR-silent, a Ni^{II} site is indicated. The lack of definite ^{61}Ni hyperfine coupling in the C_{red1} EPR signal is consistent with a C-center consisting of a Ni site isolated from the cluster.

Alternatively, the Ni may be electronically coupled to the C-cluster. Incorporation of Ni changes the properties of the Fe_4S_4 cluster in a major way. The spin state of the reduced cluster changes from $S = 3/2$ to $S = 1/2$, and one of the iron sites, FCII, acquires a special coordination. Moreover, the addition of Ni causes a substantial increase of the redox potential of the cluster; the midpoint potential of the C_{ox}/C_{red1} couple is at least 300 mV higher than that of the C^*_{ox}/C^*_{red} couple,[52] suggesting that the environment of the Fe_4S_4 core is altered. Finally, the C-cluster, unlike C*, binds CN^-. While these changes could be explained by a conformational change occurring when the Ni site becomes occupied, two spectroscopic observations by S. W. Ragsdale and co-workers[21,24] suggest an incipient covalent link between the Ni and the Fe_4S_4 cluster. First, freeze-quench resonance Raman experiments by Qiu et al.[24] have shown that a Ni-sensitive band at 365 cm^{-1} and an Fe−S band at 353 cm^{-1} disappear on the time scale (10 ms) of the appearance of C_{red2} when *as-isolated* $CODH_{Ct}$ is reduced by CO. Qiu et al. have concluded that "Ni is directly involved in the chromophore electronic system, probably through a bridge to the Fe atom(s)". The resonance Raman data do not conclusively support coupling of the Ni and Fe−S cluster for the $g_{av} = 1.82$ state since the study did not establish for *as-isolated* enzyme an association of the observed resonance Raman bands with a particular state (C_{ox}, C_{red1}, or the fraction of C-clusters incapable of attaining the $g_{av} = 1.82$ state). However, the study indicates that Ni and Fe are linked in at least one of the three states. Second, it has been reported that azide[66] and thiocyanate[21] bind to the C-cluster. Binding of thiocyanide shifts the EPR spectrum from the $g_{av} = 1.82$ state

(62) Beinert, H.; Kennedy, M. C. *Eur. J. Biochem.* **1989**, *186*, 5−15. Kent, T. A.; Dreyer, J.-L.; Kennedy, M. C.; Huynh, B. H.; Emptage, M. H.; Beinert, H.; Münck, E. *Proc. Natl. Acad. Sci. U.S.A.* **1982**, *79*, 1096−1100.

(63) (a) Werst, M. M.; Kennedy, M. C.; Houseman, A. L. P.; Beinert, H.; Hoffman, B. M. *Biochemistry* **1990**, *29*, 10533−10540. (b) Kennedy, M. C.; Stout, C. D. In *Advances in Inorganic Chemistry*; Cammack, R., Sykes, A. G., Eds.; Academic Press, Inc: San Diego, 1992; pp 323−340. Lauble, H.; Kennedy, M. C.; Beinert, H.; Stout, C. D *Biochemistry* **1992**, *31*, 2735−2747.

(64) Telser, J.; Emptage, M. H.; Merkle, H.; Kennedy, M. C.; Beinert, H.; Hoffman, B. M. *J. Biol. Chem.* **1986**, *262*, 4840−4846.

(65) Belinskii, M. *Chem. Phys.* **1993**, *172*, 189−211.

to a two-component spectrum with $g_{av} = 2.15$ ($g = 2.34$, 2.067, and 2.03) and $g_{av} = 2.17$ ($g = 2.34$, 2.115, and 2.04) while azide causes a shift to $g_{av} = 2.16$ ($g = 2.34$, 2.11, and 2.04). The EPR spectra of the azide and thiocyanate adducts did not exhibit any broadening by ^{61}Ni. However, ^{57}Fe enrichment led to a noticeable (~6 G) broadening of the resonances.[21] Spectra with $g_{av} > 2$ values have not been reported for $[Fe_4S_4]^+$ clusters, and thus the g values of the azide and thiocyanate adducts are difficult to explain by assuming that the iron−sulfur cluster of the C-center is isolated.

The experimental data can be rationalized with an electronic model that considers a Ni site linked by a bridging ligand to one Fe site of the $[Fe_4S_4]^+$ cluster. The model considered below is analogous to that developed for *Escherichia coli* sulfite reductase; i.e., it considers a weak exchange coupling of one metal site (here Ni) to a cubane with strong internal exchange coupling.[67−69] An X-ray absorption study of $CODH_{Rr}$ has shown that the Ni is not part of a structure with a $NiFe_3S_4$ core.[27] The Ni edge data were found to be consistent with a distorted tetra- or pentacoordinated Ni^{II} site. This conclusion is consistent with the fact that no EPR signal attributable to Ni^{III} or Ni^{I} has been observed and that the reduction to the $g_{av} = 1.82$ state, as shown here, intimately involves an Fe−S cluster. We will adopt the view that the Ni is divalent and has $S_{Ni} = 1$.

In our model, we describe the ground state of the Ni^{II} site with the $S_{Ni} = 1$ spin Hamiltonian

$$H_{Ni} = D(S^2_{zNi} - 2/3) + E(S^2_{xNi} - S^2_{yNi}) + \beta \mathbf{S}_{Ni}\cdot\mathbf{g}^{Ni}\cdot\mathbf{H} \quad (2)$$

where D and E are the tetragonal and rhombic zero-field splitting parameters, respectively. The ground state of the $[Fe_4S_4]^+$ cluster is described by

$$H_{Fe-S} = \beta \mathbf{S}_c\cdot\mathbf{g}^{Fe-S}\cdot\mathbf{H} \quad (3)$$

We assume that the Ni^{II} site is linked by a bridging ligand to site Fe_A of the $[Fe_4S_4]^+$ cluster, and that this bridging ligand mediates a weak exchange interaction, described by

$$H_{ex} = J\mathbf{S}_{Ni}\cdot\mathbf{S}_A \quad (4)$$

where $\mathbf{S}_A$ is the spin operator of site Fe_A. We will also assume that $|J| \ll D$, that $D > 0$, and that all tensors have a common principal axis system. By restricting our considerations to the $\mathbf{S}_c = 1/2$ subspace of the cluster and by application of the Wigner−Eckart theorem, we can replace in the exchange term the site spin $\mathbf{S}_A$ by the cluster spin $\mathbf{S}_c$ to obtain $H_{ex} = j\mathbf{S}_{Ni}\cdot\mathbf{S}_c$, where j is an effective coupling constant, $j = K_i J$. A number of arguments (see Noodleman[70]) indicate that the $S = 1/2$ ground state of $[Fe_4S_4]^+$ clusters is best described by coupling the spin $S_{12} = 9/2$ of the $Fe^{II}Fe^{III}$ pair to the spin $S_{34} = 4$ of the $Fe^{II}Fe^{II}$ pair; the spin projection factor K_i is > 0 if the Ni site is coupled to an Fe atom of the $Fe^{II}Fe^{III}$ pair, and $K_i < 0$ if an Fe site of the ferrous pair is involved. With the above modification, the Hamiltonian becomes

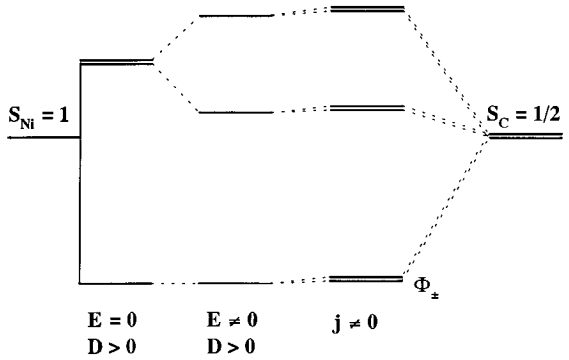

Figure 15. Energy level diagram resulting from coupling an $S_{Ni} = 1$ Ni^{II} site to the $S_c = 1/2$ ground state of an $[Fe_4S_4]^+$ cluster. The doublet $\Phi^{\pm}$ yields the $g_{av} = 1.82$ signal.

$$H = j\mathbf{S}_{Ni}\cdot\mathbf{S}_c + H_{Ni} + H_{Fe-S} \quad (5)$$

The j term couples the Fe−S cluster to the Ni^{II} site, resulting in a system consisting of three Kramers doublets separated according to the zero-field splitting of the Ni^{II} site (see Figure 15). For $j = 0$, the **g** tensor of the ground doublet is just $\mathbf{g}^{Fe-S}$. For $j \neq 0$, the exchange term mixes the two excited spin levels of the Ni^{II} into the ground doublet. We describe the Zeeman interaction of this doublet by

$$H_Z = \beta \mathbf{S}'\cdot\mathbf{g}^{eff}\cdot\mathbf{H} \quad (6)$$

where $S' = 1/2$ is an effective spin, and obtain after a simple second-order perturbation treatment for the effective g values the expressions

$$g_x^{eff} = g_x^{Fe-S} - 2g_x^{Ni}j/(D + E)$$
$$g_y^{eff} = g_y^{Fe-S} - 2g_y^{Ni}j/(D - E) \quad (7)$$
$$g_z^{eff} \approx g_z^{Fe-S}$$

Expressions 7 show how the g values can be modified by the coupling to the Ni^{II}. Unfortunately, there are eight unknowns and only three experimental g values. Nevertheless, the expressions give some valuable insights. For clarity of the following discussion, we will assume that $g_z^{Fe-S} \approx 2.0$, $g_x^{Fe-S} = g_y^{Fe-S} \approx 1.9$, and $\mathbf{g}^{Ni} = 2.0$. It can be seen that positive j values shift g_x^{eff} and g_y^{eff} downward, while negative j values can cause shifts to $g > 2.00$. The ratio $j/(D + E)$ cannot be larger than 0.05 for the $g_{av} = 1.82$ signal, suggesting that the coupling is very weak. Reported D values for Ni^{II} range from vanishingly small splittings for certain octahedral complexes to D values around +50 cm^{-1} for Ni-substituted rubredoxin and the $[Ni(SPh)_4]^{2-}$ anion.[71] These values suggest for j an upper limit of ~2 cm^{-1}. Noodleman's work[70] on the electronic structure of $[Fe_4S_4]^+$ clusters shows that the magnitudes of the spin projection factors K_i are between 1 and 2, suggesting that the magnitude of J is smaller than 2 cm^{-1} as well.

If we assume that FCII, the suggested CN^- binding site, is also the binding site for azide and thiocyanate, and if we identify FCII with the coupling site Fe_A, it is plausible that the binding of the anions changes the sign of J, leading to g_{av} values above $g = 2.0$; since J must be small, minor geometrical changes can change its sign. Finally, the model predicts also that the resonances of the $g_{av} = 1.82$ signal should not measurably

(66) Kumar, M.; Lu, W.-P.; Smith, A.; Ragsdale, S. W.; McCracken, J. *J. Am. Chem. Soc.* **1995**, *117*, 2939−2944.
(67) (a) Christner, J. A.; Münck, E.; Janick, P. A.; Siegel, L. M. *J. Biol. Chem.* **1981**, *256*, 2098−2101. (b) Christner, J. A.; Münck, E.; Janick, P. A.; Siegel, L. M. *J. Biol. Chem.* **1983**, *258*, 11147−11156. (c) Christner, J. A.; Janick, P. A.; Siegel, L. M.; Münck, E. *J. Biol. Chem.* **1983**, *258*, 11157−11164. (c) Christner, J. A.; Münck, E.; Kent, T. A.; Janick, P. A.; Salerno, J. C.; Siegel, L. M. *J. Am. Chem. Soc.* **1984**, *106*, 6786−6794.
(68) Münck, E. In *Iron Sulfur Proteins*; Spiro, T. G., Ed.; Interscience: New York, 1982; Chapter 4, pp 147−175.
(69) Bominaar, E. L.; Hu, Z.; Münck, E.; Girerd, J.-J.; Borshch, S. A. *J. Am. Chem. Soc.* **1995**, *117*, 6976−6989.
(70) Noodleman, L. *Inorg. Chem.* **1991**, *30*, 246−256. Noodleman, L. *Inorg. Chem.* **1991**, *30*, 256−264.
(71) Kowal, A. T.; Zambrano, I. C.; Moura, I.; Moura, J. J. G.; LeGall, J.; Johnson, M. K. *Inorg. Chem.* **1988**, *27*, 1162−1166.

broaden upon enrichment of CODH with ^{61}Ni. The ^{61}Ni magnetic hyperfine interaction, written as $\mathbf{S}_{Ni}\cdot\mathbf{A}^{Ni}\cdot\mathbf{I}_{Ni}$ in the language of eq 2, transforms into $\mathbf{S}'\cdot\mathbf{A}^{eff}\cdot\mathbf{I}_{Ni}$ where

$$A_x^{eff} = \{j/(D+E)\}A_x^{Ni}$$

$$A_y^{eff} = \{j/(D-E)\}A_y^{Ni} \qquad (8)$$

$$A_z^{eff} \approx 0$$

Thus, the model predicts that the components of the observed hyperfine tensor are reduced by a factor of $D/j \geq 20$ for the $g_{av} = 1.82$ state, rationalizing the lack of ^{61}Ni hyperfine broadening of the EPR resonances.

It may appear that the observed g values, $g = 1.87$, 1.78, and 1.55, of the CN^- adduct of $CODH_{Ct}$ do not fit eq 6. However, if we assume that CN^- binding causes the magnetic axes of the $[Fe_4S_4]^+$ cluster to rotate such that the direction of one of the smaller g values, say $g \approx 1.87$, is along the z axis defined by the Ni^{II} site, the g value pattern observed for the CN^- adduct can be explained as well. For $[Fe_4S_4]^+$ model complexes, a change of the magnetic axes has been observed even without addition of external ligands.[72] Alternatively, if cyanide is bridging between the cluster and the Ni^{II} site, a possibility we cannot exclude, the magnetic axes of the Ni^{II} site may reorient.

Compared to the potentials of typical $[Fe_4S_4]^{1+/2+}$ clusters, the C_{ox}/C_{red1} redox potentials (Table 1) are quite high. While the protein may modify the intrinsic potential of the C-center by minimizing formation of hydrogen bonds to the cluster or by providing a dielectric environment promoting a higher potential, replacement of cysteine as a cluster ligand by a neutral base may raise the redox potential considerably, as amply demonstrated for synthetic Fe_4S_4 clusters.[73] For instance, if the Ni and the cluster would share a bridging cysteinyl residue and if the FCII site would coordinate neutral ligands rather than a negative cysteinyl residue, the decrease of the negative cluster charge by about 1.5 could raise the potential considerably.

Spin Quantitation and Heterogeneity. One of the most puzzling aspects of CODH research has been the observation that the spin concentrations of the various $S = 1/2$ EPR signals are substantially below 1 spin/mol. For $CODH_{Ct}$, the $g_{av} = 1.82$ and 1.86 signals of the C-cluster and the NiFeC signal of the A-cluster each quantify to only 0.1−0.35 spin/$\alpha\beta$, while the $g = 1.94$ signal from the B-cluster quantifies to about 0.5−0.7 spin/$\alpha\beta$. For $CODH_{Rr}$, the $g = 1.94$ signal typically yields about 1 spin/mol, but the $g_{av} = 1.82$ and 1.86 signals have spin concentrations between 0.1 and 0.6 spin/mol.

The studies reported here give insight into the cause for the substoichiometric spin concentrations of the $CODH_{Rr}$ C-cluster signals. Recent studies[52] have provided the redox potential for the C_{ox}/C_{red1} and B_{ox}/B_{red} couples ($E^{\circ\prime} = -110$ and -418 mV, respectively). For the present study, samples were prepared at potentials (e.g., -300 mV) for which virtually all of the C- and B-clusters should have been in the C_{red1} and B_{ox} states, respectively. All of the B-clusters were found by Mössbauer spectroscopy and EPR to be in the B_{ox} state, as expected, but only 60% of the C-clusters were in the C_{red1} state; the other 40% were observed in an oxidized state (apparently C_{ox}, with some unknown structural difference that impedes access to the $g_{av} = 1.82$ state). Thus, the low spin concentration of the $g_{av} = 1.82$ state arises because only about 60% of the C-clusters undergo C_{ox}/C_{red1} redox transitions in accordance with $E^{\circ\prime} = -110$ mV; the remaining 40% are redox-inactive in this potential region. Thus, for unknown reasons, populations of C-clusters have different redox properties.

The $g_{av} = 1.86$ signal of *fully-reduced* $CODH_{Rr}$ also has substoichiometric spin concentrations because of heterogeneity. For the dithionite-reduced Mössbauer sample, we found that all of the C-clusters are reduced, but only about 40% are in the $S = 1/2$, $g_{av} = 1.86$ (C_{red2}) form; the other 60% are in a state with $S = 3/2$. The $S = 3/2$ form is similar to that of the precursor C*-cluster in the reduced state. Thus, the spin quantitations of the $g_{av} = 1.86$ signal give low values because only a fraction of C-clusters are in a state with spin $S = 1/2$; the remainder have $S = 3/2$.

Our understanding of the heterogeneous properties of the C-cluster is at a very elementary level. We have not yet been able to develop methods that yield the $g_{av} = 1.82$ signal with a predictable spin concentration; values between 0.1 and 0.6 spin/mol have been obtained, but we cannot generate samples with 0.6 spin/mol $g_{av} = 1.82$ signals *at will*. We have found that samples left undisturbed in our glovebox for ~15 h lost nearly all of their $g_{av} = 1.82$ signal intensity. This loss was not caused by oxidation (the box atmosphere had less than 1 ppm O_2, and adding additional dithionite did not increase the signal intensity). Very recently, we have observed that the $g_{av} = 1.82$ signal intensity of some CODH samples was recovered by incubating the sample in CO, and reoxidizing it with indigo carmine. Thus, the proportions of C-clusters present in various states do not appear to be "fixed" but are somehow dependent on sample history. The spin concentration of the $g_{av} = 1.82$ signal seems to depend, in a manner not understood, on the batch of CODH as well as on the method of preparing the state.

Because of the problems just mentioned, we hesitate to postulate that those molecules that do not attain the $g_{av} = 1.82$ state are also those that assume the $S = 3/2$ state form upon reduction with dithionite or CO. We have considered the possibility that this fraction of C-clusters lacks Ni and are actually C*-clusters, but holo-$CODH_{Rr}$ appears to contain ~8 Fe atoms and 1 Ni atom per molecule. Thus, Ni may be bound in these $CODH_{Rr}$ molecules, but bound differently than in those molecules affording the $g_{av} = 1.82$ and 1.86 EPR signals. The fact that Ni-deficient $CODH_{Rr}$ does not exhibit such heterogeneity in its C*-clusters (all of which have $S = 3/2$ in the reduced state) provides further evidence that multiple binding modes of the Ni may be at the root of the observed heterogeneity.

Finally, the redox behavior of the C-clusters at potentials below -400 mV is largely unexplored. It is not known whether C_{red1} and C_{red2} are isoelectronic states of the C-cluster or whether C_{red2} is two electrons further reduced. This study has shown that the C-cluster of $CODH_{Rr}$ reduced by CO or dithionite occurs in a mixture of three states, namely, C_{red1}, C_{red2}, and $C_{S=3/2}$. How the appearance of these states is related to the catalytic activity of the enzyme still needs to be explored.

Acknowledgment. This work was supported by grants from the National Institutes of Health, GM 22701 (to E.M.) and GM 46441 (to P.A.L.), the National Science Foundation, MCB-9406224 (to E.M.), and the Department of Energy, DE-FG02-78ER13691 (to P.W.L.). We thank David Hamilton and William K. Russell for help in purifying the ^{57}Fe-enriched preparations of $CODH_{Ct}$.

Note Added in Proof: While this paper was in press, M. Kumar and S. W. Ragsdale (*J. Am. Chem. Soc.* **1995**, *117*,

(72) Gloux, J.; Gloux, P.; Lamotte, B.; Mouesca, J. M.; Rius, G. *J. Am. Chem. Soc.* **1994**, *116*, 1953−1961.

(73) Johnson, R. W.; Holm, R. H. *J. Am. Chem. Soc.* **1978**, *100*, 5338−5344.

11604-11605) reported that *n*-butyl isocyanide is a substrate of $CODH_{Ct}$. Binding of *n*-butyl isocyanide led to the disappearance of the $g_{av} = 1.82$ signal with formation of a new signal with *g* values at 2.28 and ≈2.08; this signal has features ($g_{av} > 2.0$) similar to those discussed above for azide and thiocyanate treated enzyme. At the Seventh International Conference on Bioinorganic Chemistry, Ragsdale and co-workers (Kumar, K.; Qiu, D.; Lu, W. P.; Spiro, T. G.; Ragsdale, S. W. *J. Inorg. Biochem.* **1995**, *59*, 647) reported, on the basis of resonance Raman experiments, that CN^- appears to bridge between the Ni and the Fe−S moiety of the C-cluster. As indicated in our paper, this suggestion is compatible with the Mössbauer results.

JA9528386